J Math Chem (2015) 53:305–352
DOI 10.1007/s10910-014-0427-9

ORIGINAL PAPER

Stereoisograms for three-membered heterocycles: II. Chirality, *RS*-stereogenicity, and *ortho*-stereogenicity on the basis of the proligand-promolecule model

Shinsaku Fujita

Received: 5 August 2014 / Accepted: 4 October 2014 / Published online: 19 October 2014

Abstract The stereoisogram approach is applied to promolecules derived from an oxirane skeleton. First, the four substitution positions of the oxirane skeleton are examined under the action of the *RS*-stereoisomeric group $\mathbf{C}_{2v\tilde{\sigma}\hat{I}}$, where point groups for chirality (or enantiomeric relationships), *RS*-permutation groups for *RS*-stereogenicity (or *RS*-diastereomeric relationships), and ligand-reflection groups for sclerality (or holantimeric relationships) are integrated in a consistent way. A notation system for giving R_a/S_a-descriptors is proposed to specify the absolute configurations of oxirane derivatives on the basis of *RS*-stereogenicity (or *RS*-diastereomeric relationships) inherent in type-I, -III, or -V stereoisograms. The concept of *chirality faithfulness* is revised to give a rational judgement on whether R_a/S_a-descriptors are labelled in uppercase or lowercase letters. Pseudoasymmetry and extended pseudoasymmetry are discussed on the basis of type-V stereoisograms. Second, the stereoisomeric group $\widetilde{\mathbf{C}}_{2v\tilde{\sigma}\hat{I}}$, which is a supergroup of the *RS*-stereoisomeric group $\mathbf{C}_{2v\tilde{\sigma}\hat{I}}$, is used to characterize the *cis/trans*- or *Z/E*-isomerism, where multiple stereoisograms are introduced as graphic representations of stereoisomeric groups. The notation system of specifying *Z/E*-descriptors is modified to be applicable to oxirane derivatives by adopting *ortho*-stereogenicity (or *ortho*-diastereomeric relationships). Finally, the isoskeletal group $\widetilde{\widetilde{\mathbf{C}}}_{2v\tilde{\sigma}\hat{I}}$, which is a supergroup of the stereoisomeric group $\widetilde{\mathbf{C}}_{2v\tilde{\sigma}\hat{I}}$, is used to characterize total features of isomerism based on an oxirane skeleton. Multiple stereoisogram sets are introduced as graphic representations of such isoskeletal groups, where flowcharts for determining types of multiple stereoisogram sets are proposed.

S. Fujita (✉)
Shonan Institute of Chemoinformatics and Mathematical Chemistry,
Kaneko 479-7 Ooimachi, Ashigara-Kami-Gun, Kanagawa-Ken 258-0019, Japan
e-mail: shinsaku_fujita@nifty.com

Keywords Oxirane · Stereoisogram · *RS*-Stereoisomeric group · Stereoisomeric group · Notation

1 Introduction

The Cahn-Ingold-Prelog (CIP) system [1,2] has been widely adopted in the modern stereochemistry, as found in the IUPAC Provisional Recommendations 2004 [3]. The CIP system presumes 'stereogenic units' in order to assign stereochemical descriptors such as *R/S*-stereodescriptors and *E/Z*-descriptors, as exemplified in Fig. 1. For example, 'stereogenic centers' (i.e., 'chirality center' and 'pseudoasymmetric center') are considered as a kind of 'stereogenic units' on the basis of a tetrahedral skeleton **1** [4] and they are specified by *R/S*-stereodescriptors in terms of Rule P-91.1.1.1 or Rule P-92.1.4 of IUPAC 2004 [3]. As another kind of 'stereogenic units', 'stereogenic axes' (i.e., 'chirality axis' and 'pseudoasymmetric axis') are considered on the basis of an allene skeleton **2** [4] and they are specified by R_a/S_a-stereodescriptors in terms of Rule P-92.1.5.3 or Rule P-92.16 [3]. As a further kind of 'stereogenic units', a 'stereogenic double bond' is considered on the basis of an ethylene skeleton **3** [4] and the *cis/trans*-stereoisomerism is specified by *E/Z*-descriptors in terms of Rule P-91.2 and P-92.1.7 [3]. As for inorganic complexes, a square planar coordination system (SP-4) **4** is specified by polyhedral symbols with configuration indices in terms of Rule IR-9.3.3.3 of the IUPAC Recommendations 2005 [5].

Although the same term 'stereogenic units' is used to refer to the skeletons of ligancy 4 shown in Fig. 1, the descriptors assigned to them are different in nature. Thus, *R/S*- or R_a/S_a-stereodescriptors for **1** or **2** are concerned mainly with absolute configurations of enantiomers, although the cases of 'pseudoasymmetric units' are concerned with those of diastereomers. On the other hand, *E/Z*-descriptors for **3** or polyhedral symbols with configuration indices for **4** are concerned mainly with geometric configurations of diastereomers, although there are a few cases concerned with those of enantiomers. Moreover, all of the descriptors are concerned with enantiomers and diastereomers, which are conceptually different from each other. It follows that they are not assigned in terms of a single criterion. Note that enantiomers are correlated to each other by means of reflection operations, while diastereomers are correlated to each other by means of permutation operations. Because a single term 'stereoisomers' (or 'stereoisomerism') has been coined to refer to enantiomers and diastereomers (or enantiomerism and diastereoisomerism) collectively [6], the descriptors are misleadingly presumed to be assigned to stereoisomers as a single criterion.

The discussions in the preceding paragraphs cause several questions, which are closely related to one another:

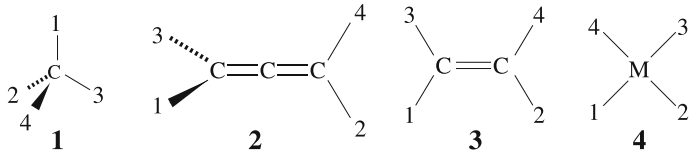

Fig. 1 Skeletons of ligancy 4 as 'stereogenic units' of the CIP system in the modern stereochemistry

1. What provides difference between **1/2** and **3/4**.
2. What provides difference between 'chiral units' (specification of enantiomers) and 'pseudoasymmetric units' (specification of diastereomers) for **1** and **2**.
3. How the term 'diastereomers' for 'pseudoasymmetric units' of **1** or **2** is different from the same term 'diastereomers' for a 'stereogenic double bond' of **3**.
4. Why all of the descriptors are concerned with enantiomers and diastereomers without a single criterion.

These questions cannot be solved so long as we obey the theoretical foundations of the modern stereochemistry, which presume a dichotomy between enantiomers and diastereomers, as recently pointed out by us [7].

In order to reorganize the theoretical foundations of stereochemistry, I have developed the stereoisogram approach [8–10], where I have proven the existence of stereoisograms of five types (type I to type V) in general [11]. The stereoisogram approach has been applied to the tetrahedral skeleton **1** [12–14] and to the allene skeleton **2** [15,16], where type-I, type-III, and type-V stereoisograms have been clarified to serve as *RS*-stereogenic cases to be specified by *R/S*- or R_a/S_a-stereodescriptors. On the other hand, the stereoisogram approach has been applied to the double-bond skeleton **3** [17] and to the square-planar skeleton **4** [18], where the concept of *m*-stereogenicity (or equivalently the concept of *m*-diastereomeric relationships) has been proposed to interpret *E/Z*-descriptors or polyhedral symbols with configuration indices (the prefix *m* means *meta* of Greek origin). The concept of *ortho*-stereogenicity (or *ortho*-diastereomeric relationships) has been proposed as a more definite concept in order to discuss the stereoisomerism of octahedral complexes [19–21]. Thus, the questions itemized above have been solved in a consistent manner.

In order to estimate the scope and limitations of the stereoisogram approach, the *RS*-stereogenicity (for **1** and **2**) and the *m*-stereogenicity (for **3** and **4**) should be compared by using other skeletons of ligancy 4. The results of Part I of this series, which has dealt with combinatorial enumeration of oxirane derivatives, provide us with many examples involving the *RS*-stereogenicity and the *m*-stereogenicity simultaneously. These are targets of the present discussions, so that the solution of the above questions will be refined in a comprehensive manner.

2 *RS*-stereoisomeric groups, stereoisomeric groups, and isoskeletal groups

2.1 *RS*-stereoisomeric group $\mathbf{C}_{2v\tilde{\sigma}\hat{I}}$

As discussed in Part I of this series, the *RS*-stereoisomeric group $\mathbf{C}_{2v\tilde{\sigma}\hat{I}}$ for characterizine an oxirane skeleton **5** is defined by starting from the point group $\mathbf{C}_{2v}$ (Fig. 2). The *RS*-stereoisomeric group $\mathbf{C}_{2v\tilde{\sigma}\hat{I}}$ (order 8) contains the following subgroups of order 4:

$$\text{point group: } \mathbf{C}_{2v} = \{I, C_2, \sigma_{v(1)}, \sigma_{v(1)}\} \tag{1}$$

$$RS\text{-permutation group: } \mathbf{C}_{2\tilde{\sigma}} = \{I, C_2, \tilde{\sigma}_{v(1)}, \tilde{\sigma}_{v(1)}\} \tag{2}$$

$$\text{ligand-reflection group: } \mathbf{C}_{2\hat{I}} = \{I, C_2, \hat{I}, \hat{C}_2\}, \tag{3}$$

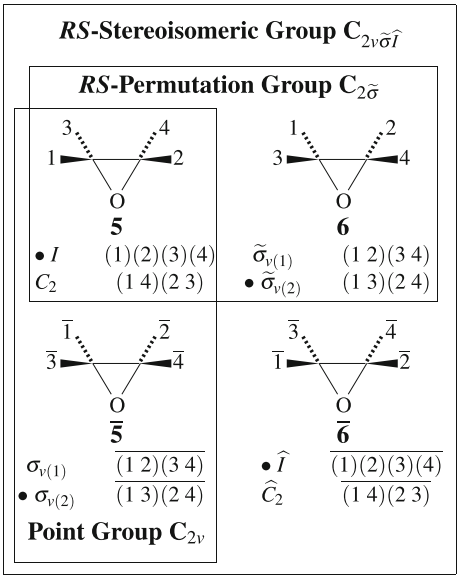

Fig. 2 Point group, *RS*-permutation group, and *RS*-stereoisomeric group for an oxirane skeleton. Each operation with a bullet symbol is selected as a representative to draw the corresponding skeleton

where they contain a common subgroup $\mathbf{C}_2$ $(= \{I, C_2\})$ corresponding to proper rotations. The four positions of the skeleton **5** are equivalent under the action of $\mathbf{C}_{2v\tilde{\sigma}\hat{I}}$, so that they construct an orbit governed by the coset representation $\mathbf{C}_{2v\tilde{\sigma}\hat{I}}(/\mathbf{C}_{\hat{I}})$, the concrete form of which is collected as products of cycles in Fig. 2. It follows that the subgroup $\mathbf{C}_{\hat{I}} = \{I, \hat{I}\}$ is the stabilizer of each position, so that the global symmetry is determined to be $\mathbf{C}_{2v\tilde{\sigma}\hat{I}}$, while the local symmetry of each position is determined to be $\mathbf{C}_{\hat{I}}$.

A quadruplet of promolecules, which are named *RS*-stereoisomers, is generated by placing an appropriate set of proligands on the four positions of the respective skeletons generated from **5** (Fig. 2), i.e., **5** (the reference skeleton), $\overline{\mathbf{5}}$ (its enantiomeric skeleton), **6** (its *RS*-diastereomeric skeleton), and $\overline{\mathbf{6}}$ (its holantimeric skeleton). Such a quadruplet in the lump is counted once in the combinatorial enumeration under the *RS*-stereoisomeric group $\mathbf{C}_{2v\tilde{\sigma}\hat{I}}$. Thereby, the number of quadruplets inequivalent under $\mathbf{C}_{2v\tilde{\sigma}\hat{I}}$ is obtained in an itemized manner with respect to a given partition (molecular formula) as well as with a subgroup of the *RS*-stereoisomeric group, as discussed in Part I of this series.

For the purpose of deriving a promolecule, a set of proligands is selected from an appropriate proligand inventory:

$$\mathbf{L} = \{\mathrm{A}, \mathrm{B}, \mathrm{X}, \mathrm{Y}; \mathrm{p}, \overline{\mathrm{p}}, \mathrm{q}, \overline{\mathrm{q}}, \mathrm{r}, \overline{\mathrm{r}}, \mathrm{s}, \overline{\mathrm{s}}\}, \tag{4}$$

where the uppercase symbols, A, B, X, and Y, denote achiral proligands, while the lowercase paired symbols, p/$\overline{\mathrm{p}}$, q/$\overline{\mathrm{q}}$, r/$\overline{\mathrm{r}}$, and s/$\overline{\mathrm{s}}$, denote chiral proligands having opposite chirality senses. The priority due to the CIP priority rule is presumed to be $\mathrm{A} > \mathrm{B} > \mathrm{X} > \mathrm{Y} > \mathrm{p} > \overline{\mathrm{p}} > \mathrm{q} > \overline{\mathrm{q}} > \mathrm{r} > \overline{\mathrm{r}} > \mathrm{s} > \overline{\mathrm{s}}$.

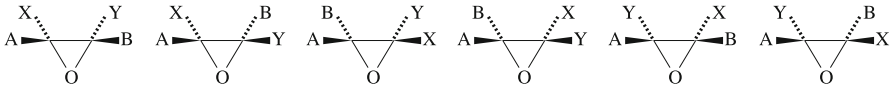

7, $[\theta]_{10}$ **8**, $[\theta]_{10}$ **9**, $[\theta]_{10}$ **10**, $[\theta]_{10}$ **11**, $[\theta]_{10}$ **12**, $[\theta]_{10}$

$\mathbf{C}_{\widehat{I}}, \mathbf{C}_1, \mathbf{C}_1, \mathrm{I}$ $\mathbf{C}_{\widehat{I}}, \mathbf{C}_1, \mathbf{C}_1, \mathrm{I}$ $\mathbf{C}_{\widehat{I}}, \mathbf{C}_1, \mathbf{C}_1, \mathrm{I}$ $\mathbf{C}_{\widehat{I}}, \mathbf{C}_1, \mathbf{C}_1, \mathrm{I}$ $\mathbf{C}_{\widehat{I}}, \mathbf{C}_1, \mathbf{C}_1, \mathrm{I}$ $\mathbf{C}_{\widehat{I}}, \mathbf{C}_1, \mathbf{C}_1, \mathrm{I}$

Fig. 3 Six oxiranes with the composition ABXY (the partition $[\theta]_{10}$), each of which is a representative of a quadruplet contained in a type-I stereoisogram. The symbols A, B, X, and Y denote proligands which are achiral in isolation (when detached). Each of the six oxiranes belongs to the *RS*-stereoisomeric group $\mathbf{C}_{\widehat{I}}$, the point group $\mathbf{C}_1$, and the *RS*-permutation group $\mathbf{C}_1$. For the partition $[\theta]_{10}$, see Part I

Note that a promolecule generated from the reference skeleton **5** can be regarded as a representative of each quadruplet in this enumeration. As for the composition ABXY, for example, there appear six representative promolecules shown in Fig. 3, where the modes of substitution are represented by substitution functions, e.g.,

$$f_1 : f_1(1) = \mathrm{A},\ f_1(2) = \mathrm{B},\ f_1(3) = \mathrm{X},\ f_1(4) = \mathrm{Y} \tag{5}$$

for generating a promolecule **7** and

$$f_2 : f_2(1) = \mathrm{A},\ f_2(2) = \mathrm{Y},\ f_2(3) = \mathrm{X},\ f_2(4) = \mathrm{B} \tag{6}$$

for generating a promolecule **8**. The mode of initial numbering of the four positions can be selected arbitrarily without losing generality.

The substitution by the set of proligands ABXY corresponds to the symmetry restriction of the original orbit of **5**. Because the resulting promolecule with ABXY belongs to $\mathbf{C}_{\widehat{I}}$, the process of the symmetry restriction is represented by the subduction of the coset representation as follows:

$$\mathbf{C}_{2v\widetilde{\sigma}\widehat{I}}(/\mathbf{C}_{\widehat{I}}) \downarrow \mathbf{C}_{\widehat{I}} = 4\mathbf{C}_{\widehat{I}}(/\mathbf{C}_{\widehat{I}}), \tag{7}$$

which is cited from Table 3 of Part I of this series. Thereby, the four positions are separated into four one-membered $\mathbf{C}_{\widehat{I}}(/\mathbf{C}_{\widehat{I}})$-orbits, each of which accommodates a proligand A, B, X, or Y according to a substitution function.

For example, the application of the substitution function f_1 to Fig. 2 generates **7** and related *RS*-stereoisomers, which construct a type-I stereoisogram shown in Fig. 4a. Note that such a type-I stereoisogram is characterized to be chiral, *RS*-stereogenic, and ascleral. The chirality is denoted by a vertical double-headed arrow with an encircled solid circle, so that a pair of **7** and $\overline{\mathbf{7}}$ (or a pair of **13** and $\overline{\mathbf{13}}$ (= **7**)) is in an enantiomeric relationship. The *RS*-stereogenicity is denoted by a horizontal double-headed arrow with an open circle, so that a pair of **7** and **13** (= $\overline{\mathbf{7}}$) (or a pair of $\overline{\mathbf{7}}$ and $\overline{\mathbf{13}}$ (= **7**)) is in an *RS*-diastereomeric relationship. The asclerality is denoted by a diagonal equality symbol with a solid circle, so that a pair of **7** and $\overline{\mathbf{13}}$ (or a pair of $\overline{\mathbf{7}}$ and **13**) is in a self-holantimeric relationship. Because of the asclerality, the enantiomeric relationship and the *RS*-diastereomeric relationship coalesce with each other.

In a similar way, the application of the substitution function f_2 to Fig. 2 generates **8** and related *RS*-stereoisomers, which construct a type-I stereoisogram shown in Fig. 4b. Similar substitution functions $f_3 - f_6$ are prepared as follows:

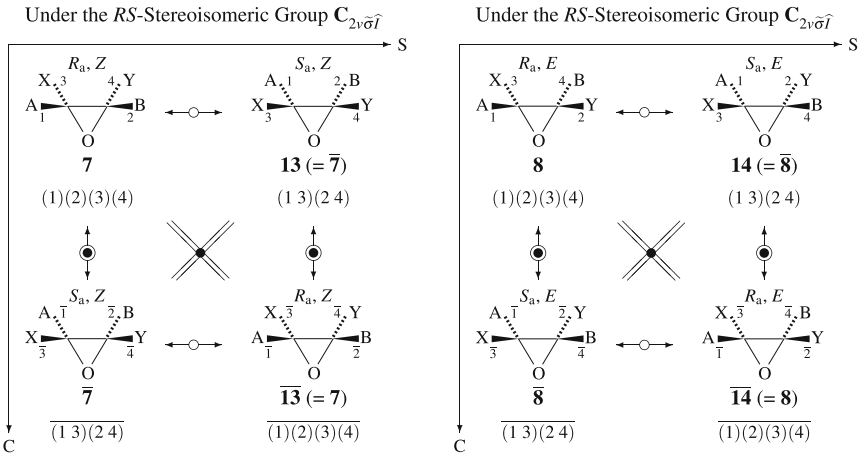

(a) $f_1 : f_1(1) = \mathrm{A}, f_1(2) = \mathrm{B}, f_1(3) = \mathrm{X}, f_1(4) = \mathrm{Y}$ **(b)** $f_2 : f_2(1) = \mathrm{A}, f_2(2) = \mathrm{Y}, f_2(3) = \mathrm{X}, f_2(4) = \mathrm{B}$

Fig. 4 Stereoisograms of type I derived from the oxirane skeleton **5**, where **a** the substitution function f_1 is applied to Fig. 2 and **b** the substitution function f_2 is applied to Fig. 2. Note that the proligands A, B, X, and Y are achiral in isolation. The reference promolecule **7** or **8** belongs to the *RS*-stereoisomeric group $\mathbf{C}_{\widehat{I}}$

$$f_3 : \; f_3(1) = \mathrm{A}, f_3(2) = \mathrm{X}, f_3(3) = \mathrm{B}, f_3(4) = \mathrm{Y} \tag{8}$$
$$f_4 : \; f_4(1) = \mathrm{A}, f_4(2) = \mathrm{Y}, f_4(3) = \mathrm{B}, f_4(4) = \mathrm{X} \tag{9}$$
$$f_5 : \; f_5(1) = \mathrm{A}, f_5(2) = \mathrm{B}, f_5(3) = \mathrm{Y}, f_5(4) = \mathrm{X} \tag{10}$$
$$f_6 : \; f_6(1) = \mathrm{A}, f_6(2) = \mathrm{X}, f_6(3) = \mathrm{Y}, f_6(4) = \mathrm{B}, \tag{11}$$

which are applied to Fig. 2. Thereby, there appear additional type-I stereoisograms, which correspond to the reference promolecules **9**–**12**.

It should be emphasized that the inequivalency between **7** and **12** under the action of the *RS*-stereoisomeric group $\mathbf{C}_{2v\widetilde{\sigma}\widehat{I}}$ is clearly demonstrated by drawing their stereoisograms, as exemplified by Fig. 4.

2.2 Stereoisomeric group $\widetilde{\mathbf{C}}_{2v\widetilde{\sigma}\widehat{I}}$

The stereoisomeric group $\widetilde{\mathbf{C}}_{2v\widetilde{\sigma}\widehat{I}}$ is defined by starting from the *RS*-stereoisomeric group $\mathbf{C}_{2v\widetilde{\sigma}\widehat{I}}$ as follows:

$$\widetilde{\mathbf{C}}_{2v\widetilde{\sigma}\widehat{I}} = \mathbf{C}_{2v\widetilde{\sigma}\widehat{I}} + \widetilde{e}\mathbf{C}_{2v\widetilde{\sigma}\widehat{I}}, \tag{12}$$

where the symbol $\widetilde{e}$ denotes an epimerization operation, which causes a pseudorotation of the 2-C-4 unit: $\widetilde{e} \sim (1)(2\,4)(3)$. The concrete operations of the stereoisomeric group $\widetilde{\mathbf{C}}_{2v\widetilde{\sigma}\widehat{I}}$ are listed in Fig. 5.

The application of the substitution function f_1 (Eq. 5) to Fig. 5 generates a type-I stereoisogram containing the *RS*-stereoisomers of **7** as well as another type-I stereoisogram concerning a stereoisomer due to the epimerization operation $\widetilde{e}$, i.e., **8**′. The two stereoisograms construct a multiple stereoisogram of type I–I, as shown in Fig. 6.

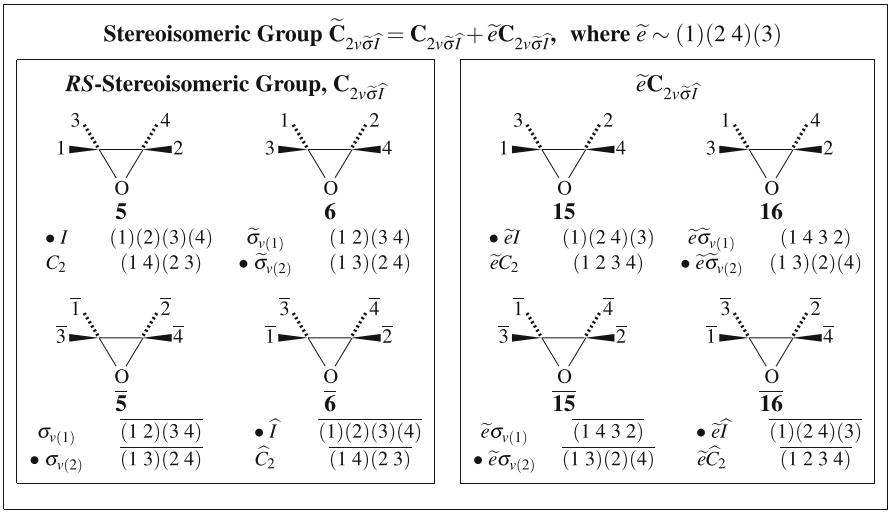

Fig. 5 *RS*-stereoisomeric group and stereoisomeric group for an oxirane skeleton. Each operation with a bullet symbol is selected as a representative to draw the corresponding skeleton

Note that the right stereoisogram of Fig. 6 is identical with the type-I stereoisogram shown in Fig. 4b, except the modes of numbering. However, the difference in the modes of numbering is conceptually important, because the former is generated under the action of the *RS*-stereoisomeric group $\mathbf{C}_{2v\widetilde{\sigma}\widehat{I}}$ (Fig. 2), while the latter is generated under the action of the stereoisomeric group $\mathbf{C}_{2v\widetilde{\sigma}\widehat{I}}$ (Fig. 5).

In a similar way, the application of the substitution function f_3 (Eq. 8) to Fig. 5 generates another multiple stereoisogram of type I–I, which represents the stereoisomerism between **9** and **10**. The multiple stereoisogram consists of two stereoisograms which characterize the *RS*-stereoisomerism concerning **9** and **10**. On the other hand, the application of the substitution function f_5 (Eq. 10) to Fig. 5 generates a further multiple stereoisogram of type I–I, which represents the stereoisomerism between **11** and **12**. The multiple stereoisogram consists of two stereoisograms which represent the *RS*-stereoisomerism concerning **11** and **12**.

It should be emphasized that stereoisomeric relationships between **7** and **8**, between **9** and **10**, as well as between **11** and **12** are elucidated by drawing multiple stereoisograms.

The two diagrams of Fig. 6 are identical with the the stereoisograms shown in Fig. 4a, b if the modes of numbering are not taken into consideration. This means that the multiple stereoisogram (Fig. 6) can be interpreted to show the relationship between the two stereoisograms (Fig. 4a, b).

The term *m-diastereomeric* coined to interpret *E/Z*-descriptors [17] is also used to refer to the relationship between such two stereoisograms contained in a multiple stereoisogram. For example, the two stereoisograms (Fig. 4a, b) are in an *m*-diastereomeric relationship in terms of the multiple stereoisogram shown in Fig. 6. Note that the two stereoisograms (Fig. 4a, b) are inequivalent under the *RS*-stereoisomeric group $\mathbf{C}_{2v\widetilde{\sigma}\widehat{I}}$ (cf. Part I of this series), but they are equivalent (i.e., convertible) under the stereoisomeric group $\widetilde{\mathbf{C}}_{2v\widetilde{\sigma}\widehat{I}}$ (Fig. 6).

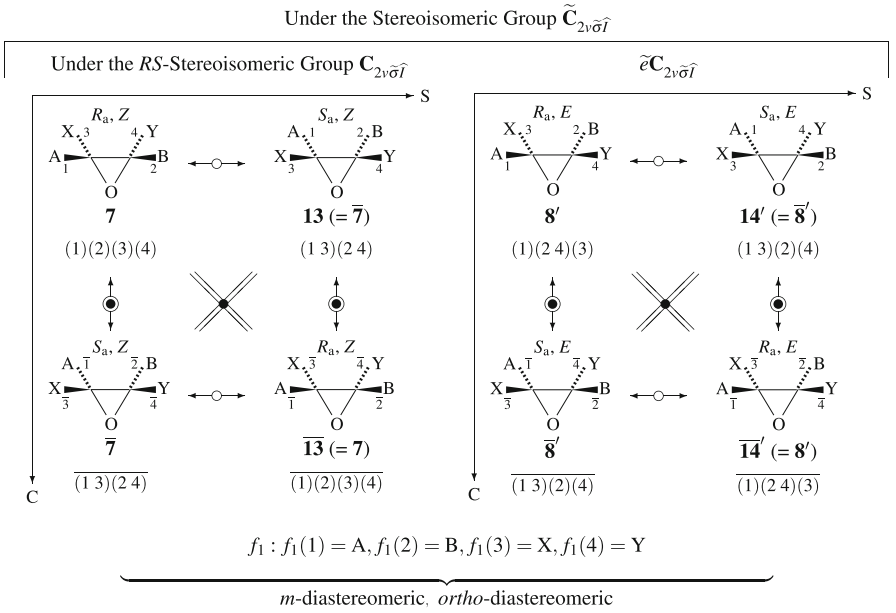

Fig. 6 Multiple stereoisogram of type I–I derived from the oxirane skeleton **5**, where the substitution function f_1 is applied to Fig. 5. Note that the proligands A, B, X, and Y are achiral in isolation

In more complicated cases, the ex-chiral subgroup (e.g., $\widetilde{\mathbf{C}}_{2\widetilde{\sigma}}$) of a stereoisomeric group (e.g., $\widetilde{\mathbf{C}}_{2v\widetilde{\sigma}\widehat{\imath}}$) can be used [20] under the name of *stereo-permutation group*. Let us collect ex-chiral operations among the operations of the stereoisomeric group $\widetilde{\mathbf{C}}_{2v\widetilde{\sigma}\widehat{\imath}}$ (Eq. 12). Then we obtain the following stereo-permutation group as an ex-chiral subgroup of order 8:

$$\widetilde{\mathbf{C}}_{2\widetilde{\sigma}} = \mathbf{C}_{2\widetilde{\sigma}} + \widetilde{e}\mathbf{C}_{2\widetilde{\sigma}}, \tag{13}$$

where $\mathbf{C}_{2\widetilde{\sigma}}$ is the *RS*-permutation group shown in Fig. 2. Then, two promolecules equivalent under the stereo-permutation group $\widetilde{\mathbf{C}}_{2\widetilde{\sigma}}$ but inequivalent under the *RS*-permutation group $\mathbf{C}_{2\widetilde{\sigma}}$ is referred to as being in an *ortho*-diastereomeric relationship. For example, **7** (Fig. 4(a)) and **8** (Fig. 4(b)) are *ortho*-diastereomeric to each other, because they are equivalent under the stereo-permutation group $\widetilde{\mathbf{C}}_{2\widetilde{\sigma}}$ (cf. **8** = **8′** in Fig. 6). Because **7** and $\overline{\mathbf{8}}$ (= $\overline{\mathbf{8}}'$) are inequivalent under the stereo-permutation group $\widetilde{\mathbf{C}}_{2\widetilde{\sigma}}$, the relationship between them should be replaced by the relationship between the corresponding stereoisograms (Fig. 4(a) vs. (b)), which is referred to as being *m*-diastereomeric.

2.3 Isoskeletal group $\widetilde{\widetilde{\mathbf{C}}}_{2v\widetilde{\sigma}\widehat{\imath}}$

The isoskeletal group $\widetilde{\widetilde{\mathbf{C}}}_{2v\widetilde{\sigma}\widehat{\imath}}$ is defined by starting from the stereoisomeric group $\widetilde{\mathbf{C}}_{2v\widetilde{\sigma}\widehat{\imath}}$, which, in turn, has been defined by Eq. 12. Let the symbols $\widetilde{s}$ and $\widetilde{\widetilde{s}}$ denote

isoskeletal permutations, which causes a switching of relevant bonds: $\widetilde{s} \sim (1)(2\,3)(4)$ and $\widetilde{\widetilde{s}} \sim (1)(2)(3\,4)$. Then, the isoskeletal group $\widetilde{\widetilde{\mathbf{C}}}_{2v\widetilde{\sigma}\widehat{I}}$ is defined as follows:

$$\widetilde{\widetilde{\mathbf{C}}}_{2v\widetilde{\sigma}\widehat{I}} = \widetilde{\mathbf{C}}_{2v\widetilde{\sigma}\widehat{I}} + \widetilde{s}\widetilde{\mathbf{C}}_{2v\widetilde{\sigma}\widehat{I}} + \widetilde{\widetilde{s}}\widetilde{\mathbf{C}}_{2v\widetilde{\sigma}\widehat{I}}, \tag{14}$$

the order of which is equal to 48 ($= 16 \times 3$). The concrete operations of the isoskeletal group $\widetilde{\widetilde{\mathbf{C}}}_{2v\widetilde{\sigma}\widehat{I}}$ are listed in Fig. 7.

In a similar way to the construction of the isoskeletal group $\widetilde{\widetilde{\mathbf{C}}}_{2v\widetilde{\sigma}\widehat{I}}$ (Eq. 14), we obtain the following group of order 24 by starting from $\widetilde{\mathbf{C}}_{2\widetilde{\sigma}}$ (Eq. 13):

$$\widetilde{\widetilde{\mathbf{C}}}_{2\widetilde{\sigma}} = \widetilde{\mathbf{C}}_{2\widetilde{\sigma}} + \widetilde{s}\widetilde{\mathbf{C}}_{2\widetilde{\sigma}} + \widetilde{\widetilde{s}}\widetilde{\mathbf{C}}_{2\widetilde{\sigma}}, \tag{15}$$

which is a subgroup of $\widetilde{\widetilde{\mathbf{C}}}_{2v\widetilde{\sigma}\widehat{I}}$. The subgroup $\widetilde{\widetilde{\mathbf{C}}}_{2\widetilde{\sigma}}$ called an *isoskeletal-permutation group* (Eq. 15) is isomorphic to the symmetric group of degree 4 ($\mathbf{S}^{[4]}$).

The application of the substitution function f_1 (Eq. 5) to Fig. 7 generates a multiple stereoisogram set of type I–I/I–I/I–I shown in Fig. 8, which contains isoskeletomers of **7** due to the isoskeletal permutations $\widetilde{s}$ and $\widetilde{\widetilde{s}}$. The multiple stereoisogram set of type I–I/I–I/I–I (Fig. 8) is based on the multiple stereoisogram shown in Fig. 6, which is in turn based on the stereoisogram shown in Fig. 4a.

2.4 Classification of various isomers by equivalence classes

In general, the concept of *equivalence classes* (orbits) is a key for discussing stereochemistry and stereoisomerism. In the present case, the following nested appearance of equivalence classes should be taken into consideration:

1. (Equivalence classes under the isoskeletal group $\widetilde{\widetilde{\mathbf{C}}}_{2v\widetilde{\sigma}\widehat{I}}$) The multiple stereoisogram set of type I–I/I–I/I–I (Fig. 8) indicates an equivalence class under the action of the isoskeletal group $\widetilde{\widetilde{\mathbf{C}}}_{2v\widetilde{\sigma}\widehat{I}}$ (Fig. 7). Note that a single substitution function f_1 (Eq. 5) is used during the derivation process of the multiple stereoisogram set shown in Fig. 8.
2. (Equivalence classes under the stereoisomeric group $\widetilde{\mathbf{C}}_{2v\widetilde{\sigma}\widehat{I}}$) From the stereoisomeric point of view, on the other hand, the multiple stereoisogram set of type I–I/I–I/I–I can be interpreted to consist of three multiple stereoisograms of type I–I, each of which indicates an equivalence class under the action of the stereoisomeric group $\widetilde{\mathbf{C}}_{2v\widetilde{\sigma}\widehat{I}}$ (Fig. 5). The top multiple stereoisogram of type I–I (concerning **7** etc.) is generated by the application of the substitution function f_1 (Eq. 5) to Fig. 5 (cf. Fig. 6). The middle multiple stereoisogram of type I–I (concerning **9** etc.) can be generated by the application of the substitution function f_3 (Eq. 8) to Fig. 5, although the mode of numbering is different. The bottom multiple stereoisogram of type I–I (concerning **11** etc.) is generated by the application of the substitution function f_5 (Eq. 10) to Fig. 5, although the mode of numbering is different.
3. (Equivalence classes under the *RS*-stereoisomeric group $\mathbf{C}_{2v\widetilde{\sigma}\widehat{I}}$) The multiple stereoisogram set of type I–I/I–I/I–I can be interpreted to consist of six stereoisograms of type I, each of which indicates an equivalence class under the action

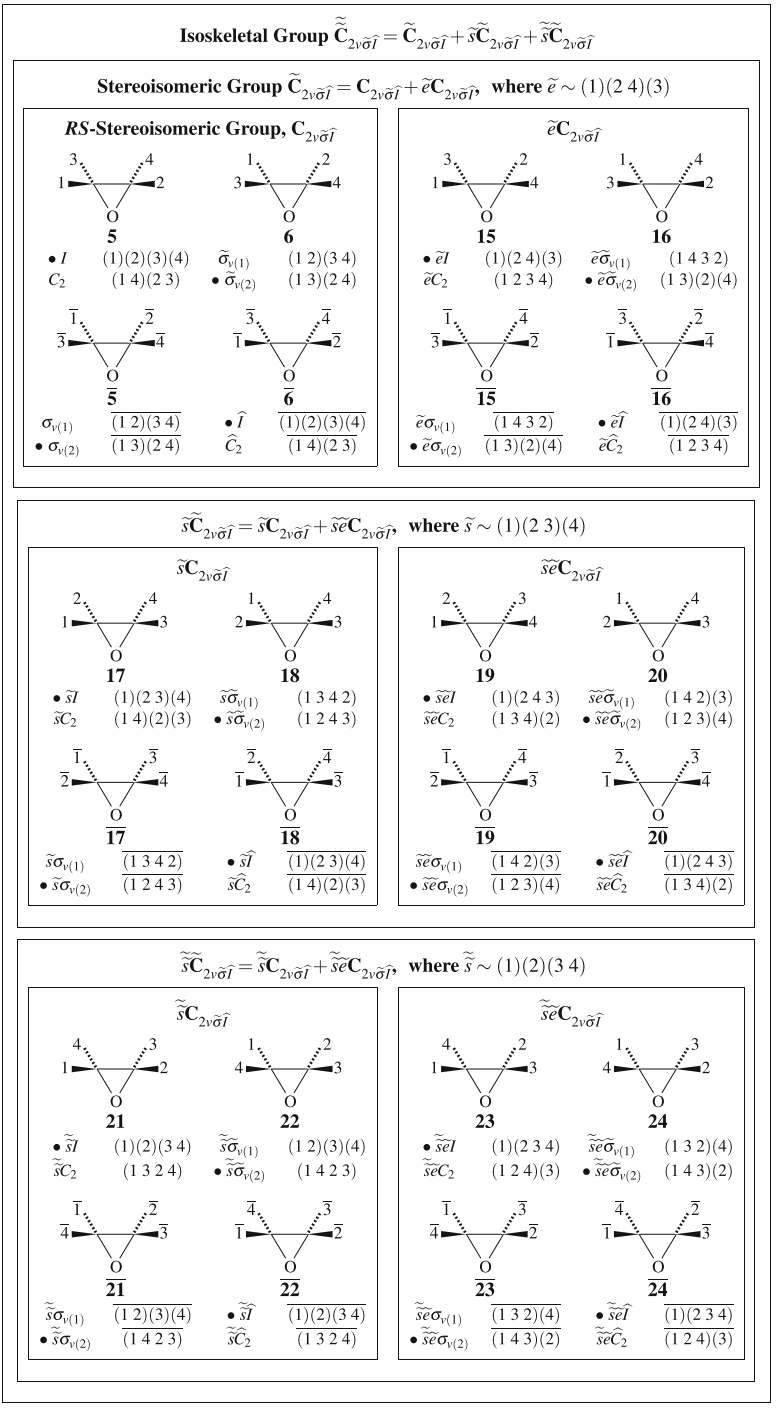

Fig. 7 *RS*-Stereoisomeric groups, stereoisomeric groups, and isoskeletal groups for an oxirane skeleton. Each operation with a bullet symbol is selected as a representative to draw the corresponding skeleton

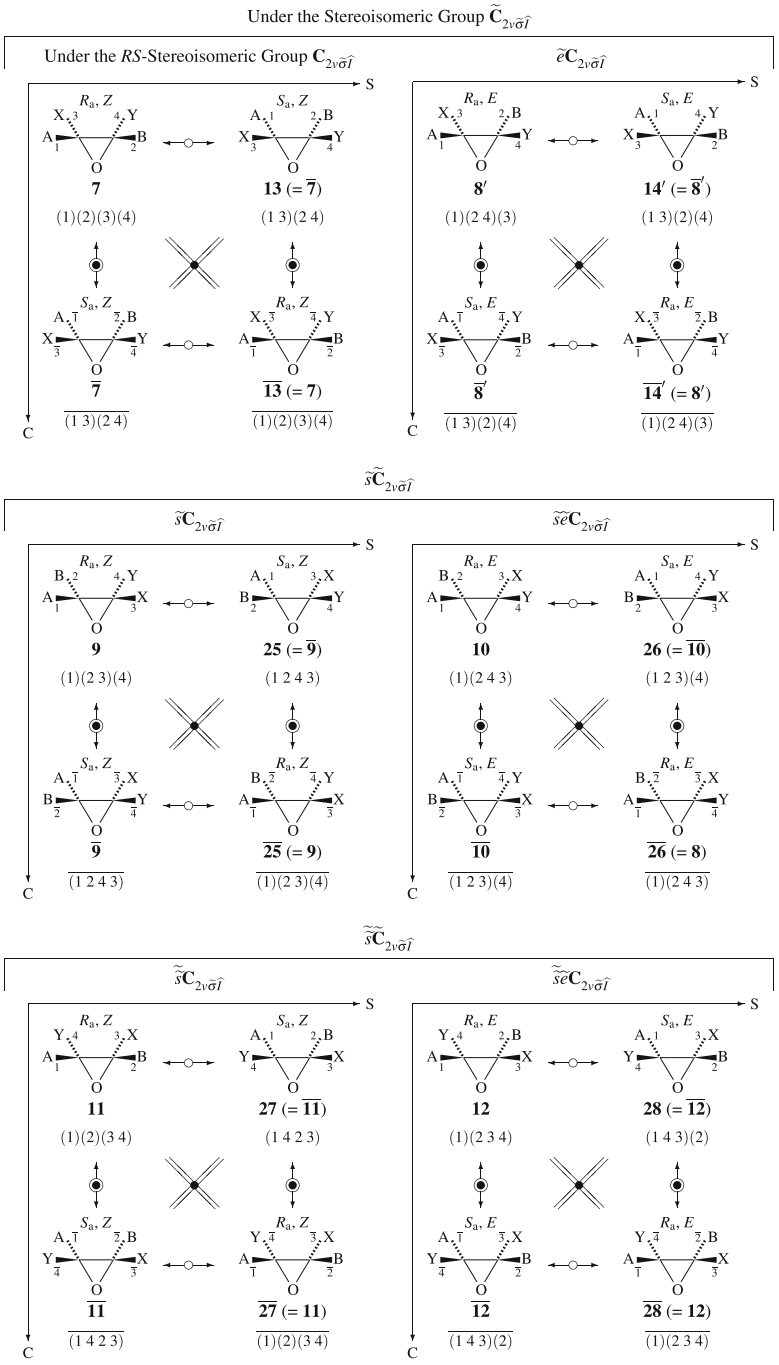

Fig. 8 Multiple stereoisogram set of type I–I/I–I/I–I derived from the oxirane skeleton **5**, where the substitution function f_1 is applied to Fig. 7. Note that the proligands A, B, X, and Y are achiral in isolation

of the *RS*-stereoisomeric group $\mathbf{C}_{2v\tilde{\sigma}\hat{I}}$ (Fig. 2). The first stereoisogram of Fig. 8 (concerning **7**) is generated by the application of the substitution function f_1 (Eq. 5) to Fig. 2 (cf. Fig. 4a). The second stereoisogram of Fig. 8 (concerning **8**) is generated by the application of the substitution function f_2 (Eq. 6) to Fig. 2 (cf. Fig. 4b). In similar ways, the the applications of the substitution functions f_3-f_6 (Eqs. 8-11) generate the remaining stereoisograms of Fig. 8 (concerning **9**, **10**,**11**, and **12**).

It should be noted that the relevant groups are nested, i.e., $\tilde{\tilde{\mathbf{C}}}_{2v\tilde{\sigma}\hat{I}} \supset \tilde{\mathbf{C}}_{2v\tilde{\sigma}\hat{I}} \supset \mathbf{C}_{2v\tilde{\sigma}\hat{I}}$. In contrast, the three subgroups of the *RS*-stereoisomeric group $\mathbf{C}_{2v\tilde{\sigma}\hat{I}}$, i.e., the point group $\mathbf{C}_{2v}$ (for enantiomeric relationships), the *RS*-permutation group $\mathbf{C}_{2\tilde{\sigma}}$ (for *RS*-diastereomeric relationships), and the ligand-reflection group $\mathbf{C}_{2\hat{I}}$ (for holantimeric relationships), do not exhibit nested nature but overlap each other partially at the chiral point group $\mathbf{C}_2$.

2.5 Flowchart for determining types of multiple stereoisogram sets

The discussions in the preceding paragraph are summarized to give a flowchart shown in Fig. 9, which is capable of classifying various kinds of isomers on the basis of equivalence classes.

For example, the promolecules collected in Fig. 3 and their enantiomers (**7**/$\overline{\mathbf{7}}$–**12**/$\overline{\mathbf{12}}$) as well as relevant promolecules represented by ABX≡C—(C=O)—Y, ABY≡C—(C=O)—X, etc. are considered to be isomers with a molecular formula C_2OABXY. They have the same rational formula C_2OABXY, where the unit C_2O is regarded as an abstract skeleton, which consist of an oxirane skeleton and a skeleton represented by ≡C—(C=O)—. The molecular formula for characterizing isomers is denoted simply by the composition ABXY or by the partition $[\theta]_{10}$, as described in Part I.

1. The first step of judgement in terms of the isoskeletal group $\tilde{\tilde{\mathbf{C}}}_{2v\tilde{\sigma}\hat{I}}$ (Fig. 7) indicates that the former set of promolecules (**7**/$\overline{\mathbf{7}}$– **12**/$\overline{\mathbf{12}}$), which are generated from the oxirane skeleton, constructs an equivalence class of isoskeletomers surrounded by a pair of braces (Fig. 9). The multiple stereoisogram set of type I–I/I–I/I–I (Fig. 8) is drawn for the purpose of systematic examination. Another isoskeletal group for characterizing a skeleton represented by ≡C—(C=O)— should be applied to remaining promolecules. The relationship between two equivalence classes of isoskeletomers, each of which is surrounded by a pair of braces, is referred to as being *skeletally-anisomeric*.
2. The second step of judgement in terms of the stereoisomeric group $\tilde{\mathbf{C}}_{2v\tilde{\sigma}\hat{I}}$ (Fig. 5) indicates that the equivalence class ({**7**/$\overline{\mathbf{7}}$–**12**/$\overline{\mathbf{12}}$}) under $\tilde{\tilde{\mathbf{C}}}_{2v\tilde{\sigma}\hat{I}}$ is divided into a set of equivalence classes under $\tilde{\mathbf{C}}_{2v\tilde{\sigma}\hat{I}}$, i.e., $\langle$**7**/$\overline{\mathbf{7}}$, **8**/$\overline{\mathbf{8}}\rangle$, $\langle$**9**/$\overline{\mathbf{9}}$, **10**/$\overline{\mathbf{10}}\rangle$, and $\langle$**11**/$\overline{\mathbf{11}}$, **12**/$\overline{\mathbf{12}}\rangle$. Note that the three equivalence classes are inequivalent to one another under the stereoisomeric group $\tilde{\mathbf{C}}_{2v\tilde{\sigma}\hat{I}}$, where the relationship between one pair of angle brackets and another pair of angle brackets is referred to as being *constitutionally-isometric*. For the purpose of systematic examination, a multiple stereoisogram such as Fig. 6 is useful.

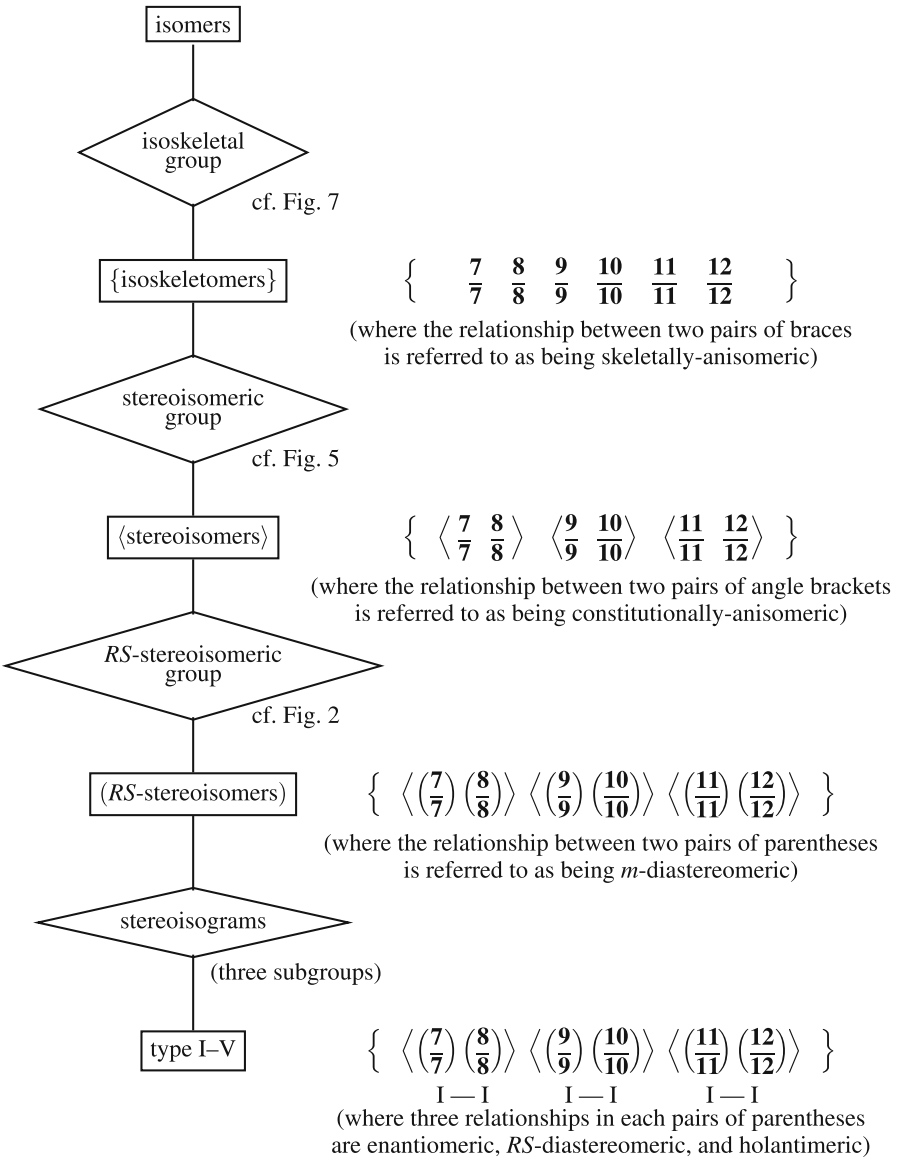

Fig. 9 Flowchart for classifying various kinds of isomers on the basis of equivalence classes. A pair of braces represents isoskeletal isomers as an equivalence class under an isoskeletal group (e.g., Fig. 7), a pair of brackets represents stereoisomers as an equivalence class under a stereoisomeric group (e.g., Fig. 5), and a pair of parentheses represents *RS*-stereoisomers as an equivalence class under an *RS*-stereoisomeric group (e.g., Fig. 2). The judgement based on stereoisograms uses the combination of equivalence classes due to three subgroups of the *RS*-stereoisomeric group, i.e., a point group, an *RS*-permutation group, and a ligand-reflection group

3. The third step of judgement in terms of the *RS*-stereoisomeric group $\mathbf{C}_{2v\tilde{\sigma}\hat{I}}$ (Fig. 2) indicates that each of the equivalence class $\langle \mathbf{7}/\overline{\mathbf{7}}, \mathbf{8}/\overline{\mathbf{8}} \rangle$, etc. under $\mathbf{C}_{2v\tilde{\sigma}\hat{I}}$ is divided into a set of equivalence classes under $\mathbf{C}_{2v\tilde{\sigma}\hat{I}}$, e.g., $\left(\mathbf{7}/\overline{\mathbf{7}}\right)$ and $\left(\mathbf{8}/\overline{\mathbf{8}}\right)$. This step of judgement is conducted schematically by drawing stereoisograms such as Fig. 4a, b. The relationship between one pair of parentheses $\left(\mathbf{7}/\overline{\mathbf{7}}\right)$ and another pair of parentheses $\left(\mathbf{8}/\overline{\mathbf{8}}\right)$ is referred to as being *m*-diastereomeric. The relationship between the promolecules **7** and **8** (or between $\overline{\mathbf{7}}$ and $\overline{\mathbf{8}}$) is referred to as being *ortho*-diastereomeric.
4. Each equivalence class under $\mathbf{C}_{2v\tilde{\sigma}\hat{I}}$ (e.g., $\left(\mathbf{7}/\overline{\mathbf{7}}\right)$) corresponds to a stereoisogram, which is examined in the 4th step of judgement. Because the *RS*-stereoisomeric group $\mathbf{C}_{2v\tilde{\sigma}\hat{I}}$ contains three subgroups, i.e., the point group $\mathbf{C}_{2v}$, the *RS*-permutation group $\mathbf{C}_{2\tilde{\sigma}}$, and the ligand-reflection group $\mathbf{C}_{2\hat{I}}$, the 4th judgement uses the combination of equivalence classes due to these three subgroups. Thereby each equivalence class under $\mathbf{C}_{2v\tilde{\sigma}\hat{I}}$ is categorized into type I to type V. The type I–I/I–I/I–I is elucidated to denote the multiple stereoisogram set at issue (Fig. 8). It should be noted that the chiral point group $\mathbf{C}_2$ is a common subgroup for the point group $\mathbf{C}_{2v}$, the *RS*-permutation group $\mathbf{C}_{2\tilde{\sigma}}$, and the ligand-reflection group $\mathbf{C}_{2\hat{I}}$, so that it serves as a group for examining homomeric relationships.

As enumerated in Part I of this series, each partition of $[\theta]_i$ ($i = 1$–30) corresponds maximally to six promolecules categorized into five types. These promolecules serve as representatives for construction a multiple stereoisogram set, the type of which is elucidated by using the flowchart shown in Fig. 9, as summarized in Table 1. Note that the type I–I/I–I/I–I for the multiple stereoisogram set for ABXY ($[\theta]_{10}$) appears in the $[\theta]_{10}$-row of Table 1.

If we focus our discussions on geometric aspects of stereochemistry, the judgement by means of stereoisograms in the 4th step of the flowchart (Fig. 9) can be replaced by the sole use of a point group, as shown in Fig. 10a. Thereby, pairs of (self-)enantiomers are regarded as equivalence classes. Note that a pair of self-enantiomers is an achiral promolecule. It follows that a pair of enantiomers or an achiral promolecule is regarded as an equivalence class, so as to be counted once under the action of a point group. Thus, a type-I or type-II stereoisogram corresponds to one pair of enantiomers; a type-IV stereoisogram corresponds to one achiral promolecule; a type-III stereoisogram corresponds to two pairs of enantiomers; and a type-V stereoisogram corresponds to two achiral promolecules.

The relationship between two pairs of enantiomers for type III or between two achiral promolecules of type V can be characterized by the term *RS-diastereomeric*, where the original meaning for characterizing the relationship between two promolecules is extended to characterize the relationship between two pairs of (self-)enantiomers. Note that one pair of enantiomers for type I or II can be regarded as a coincident case between enantiomeric relationships and *RS*-diastereomeric ones. For example, the symbol $\left(\mathbf{7}/\overline{\mathbf{7}}\right)$ corresponds to one quadruplet of a type-I stereoisogram under the *RS*-stereoisomeric group $\mathbf{C}_{2v\tilde{\sigma}\hat{I}}$ (due to the flowchart shown in Fig. 9) and corresponds to one pair of enantiomers under the point group $\mathbf{C}_{2v}$ (due to the flowchart shown in Fig. 10a). This case is regarded as a coincident case between an enantiomeric rela-

Table 1 Types of multiple stereoisogram sets for oxirane Promolecules

Partition $[\theta]_i$	Representative compositions	Type	Assignability of Ra/Sa	Assignability of Z/E	Example
$[\theta]_1$	A^4	$(IV^2)^3$	N	N	
$[\theta]_2$	A^3B	$(I^2)^3$	Y	N	Fig. 29
$[\theta]_3$	A^3p	$(III^2)^3$	Y	N	Fig. 30
$[\theta]_4$	A^2B^2	$(I–IV)^2/IV^2$	Y-N/N	Y/N	Fig. 18
$[\theta]_5$	A^2p^2	$(III–II)^2/II^2$	Y-N/N	Y/N	Fig. 20
$[\theta]_6$	A^2BX, ABX^2	$(I–I)^2/I^2$	Y-Y/Y	Y/N	Fig. 22
$[\theta]_7$	A^2Bp	$(III–III)^2/III^2$	Y-Y/Y	Y/N	Fig. 24
$[\theta]_8$	$A^2p\bar{p}$	$(I–V)^2/V^2$	Y-Y/Y	Y/N	Fig. 26
$[\theta]_9$	A^2pq	$(III–III)^2/III^2$	Y-Y/Y	Y/N	
$[\theta]_{10}$	ABXY	I–I/I–I/I–I	Y–Y/Y–Y/Y–Y	Y/Y/Y	Fig. 8
$[\theta]_{11}$	ABXp	III–III/III–III/III–III	Y–Y/Y–Y/Y–Y	Y/Y/Y	Fig. 14
$[\theta]_{12}$	ABp2	$(III–III)^2/III^2$	Y–Y/Y	Y/N	
$[\theta]_{13}$	AB$p\bar{p}$	$(III–III)^2$/III=III	Y-Y/Y(†)	Y/Y*	(Fig. 32)
$[\theta]_{14}$	ABpq	III–III/III–III/II1–III	Y–Y/Y–Y/Y–Y	Y/Y/Y	
$[\theta]_{15}$	Ap^3	$(III^2)^3$	Y	N	
$[\theta]_{16}$	A$\bar{p}^2$p	$(III–III)^2/III^2$	Y(†)-Y(†)/Y	Y*/N	
$[\theta]_{17}$	Ap^2q	$(III–III)^2/III^2$	Y–Y/Y	Y/N	
$[\theta]_{18}$	Ap$\bar{p}$q	III–III/III–III/II1–III	Y–Y/Y–Y/Y(†)–Y(†)	Y/Y/Y*	
$[\theta]_{19}$	Apqr	III–III/III–III/II1–III	Y–Y/Y–Y/Y–Y	Y/Y/Y	
$[\theta]_{20}$	p^4	$(II^2)^3$	N	N	
$[\theta]_{21}$	$p^3\bar{p}$	$(III^2)^3$	Y†	N	Fig. 31
$[\theta]_{22}$	pq	$(III^2)^3$	Y	N	
$[\theta]_{23}$	$p^2\bar{p}^2$	$(V–IV)^2/IV^2$	Y–N/N	Y/N	Fig. 28
$[\theta]_{24}$	$p^2\bar{p}q$	$(III–III)^2/III^2$	Y†-Y†/Y	Y*/N	
$[\theta]_{25}$	p^2q^2	$(III–II)^2/II^2$	Y–N/N	Y/N	
$[\theta]_{26}$	$p^2q\bar{q}$	$(III–III)^2/III^2$	Y†-Y/Y†	Y/N	
$[\theta]_{27}$	p^2qr	$(III–III)^2/III^2$	Y–Y/Y	Y/N	
$[\theta]_{28}$	p$\bar{p}$q$\bar{q}$	I–V/I–V/V–V	Y–Y/Y–Y/Y–Y	Y/Y/Y	Fig. 16
$[\theta]_{29}$	p$\bar{p}$qr	III–III/III–III/III–III	Y–Y/Y–Y/Y–Y	Y/Y*/Y	
$[\theta]_{30}$	pqrs		Y–Y/Y–Y/Y–Y	Y/Y/Y	

* Exhibiting special features. † Chirality-unfaithful for type III

tionship and an *RS*-diastereomeric one, as found in the type-I stereoisogram shown in Fig. 4a.

It is here worthwhile to mention the difference between the modern stereochemistry and the stereoisogram approach from a viewpoint of methodology. Many flowcharts for determining isometric relationships have been reported in articles (cf. Flowchart 1 of [22] and the flowchart of [23]) and textbooks on stereochemistry (cf. Fig. 4.12 of

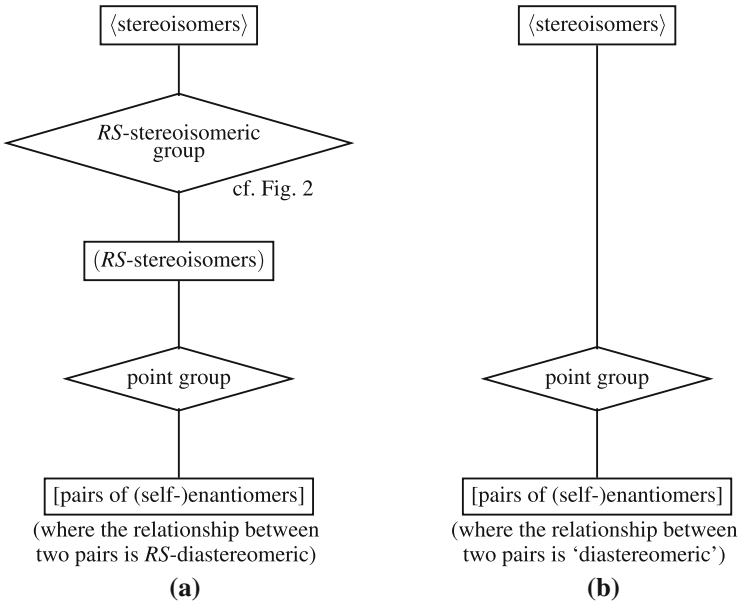

Fig. 10 Modified flowcharts for classifying various kinds of isomers on the basis of equivalence classes **a** due to the stereoisogram approach and **b** due to the modern stereochemistry

[24] and Fig. 4.3 of [25]). If you search WEB by using such a keyword as 'flowchart, stereoisomer', you would find further more flowcharts for isomer determination, e.g., a flowchart shown in the term 'Isomer' from Wikipedia [26].

Although these conventional flowcharts exhibit different appearances, they are commonly based on structural difference between two molecules, where nonsuperposable mirror images are determined to be in an enantiomeric relationship. For the purpose of a more definite comparison upon a common basis, the step for detecting nonsuperposable mirror images in the conventional flowcharts is replaced by the step using equivalence classes under a point group. Thereby, the conventional flowcharts can be modified into a flowchart shown in Fig. 10b.

The comparison shown in Fig. 10 indicates that the flowchart of Fig. 10b of the modern stereochemistry lacks equivalence classes based on the *RS*-stereoisomeric group. In other words, the the conventional flowcharts implicitly select point groups from the three subgroups of *RS*-stereoisomeric groups and neglect *RS*-permutation groups and ligand-reflection groups. This implicit selection results in the dichotomy between enantiomers and diastereomers in the modern stereochemistry, i.e., "stereoisomeric relationships other than enantiomeric relationship are referred to as diastereomeric relationships". Note that the relationship between two pairs of (self-)enantiomers in Fig. 10b (i.e., under the terminology of the modern stereochemistry) is 'diastereomeric', while the relationship between two pairs of (self-)enantiomers is *RS*-diastereomeric in Fig. 10a (i.e., under the terminology of the stereoisogram approach).

The apparent success concerned with the flowchart of Fig. 10b (and the conventional flowcharts described above in the modern stereochemistry) should be pointed out to be rather fortunate. Thus, the apparent success stems from the fact the *RS*-stereoisomeric groups are coincident with the stereoisomeric groups in case of the 'stereogenic units' **1** and **2**; as well as from the fact that the *RS*-stereoisomeric groups are coincident with the point groups in case of the 'stereogenic double bond' **3** and the square planar coordination system (SP-4) **4**. In contrast, the present case of oxirane derivatives reveals the necessity of *RS*-stereoisomeric groups for comprehensive discussions on stereochemistry and stereoisomerism.

3 Stereochemical notations

3.1 Specification of absolute configurations

If promolecules based on the tetrahedral skeleton **1** or on the allene skeleton **2** are characterized by type-I, type-III, or type-V stereoisograms, their absolute configurations are designated by *R/S*- or R_a/S_a-stereodescriptors, which are assigned by means of *RS*-diastereomeric relationships (not by means of enantiomeric relationships). In a similar way, promolecules based on the oxirane skeleton **5** should be distinguished by an appropriate system of stereodescriptors, if they are determined to have type-I, type-III, or type-V stereoisograms.

However, the modern stereochemistry lacks such an appropriate system of stereodescriptors, so that *R/S*-stereodescriptors for 'chirality centers' are separately assigned to the two carbons of an oxirane ring. This type of assignments emphasizes local symmetries and makes little of global symmetries of oxirane derivatives. Because the stereoisogram approach is able to treat the global symmetries of oxirane derivatives properly, a new system of R_a/S_a-stereodescriptors is proposed here to characterize oxiranes having type-I, type-III, or type-V stereoisograms.

The practices for determining the order of precedence in the CIP system [1–3] are applied to the four proligands of an oxirane promolecule, where the set of two proligands (a and b) on one carbon has the order of precedence $a > b$ and the set of two proligands on the other carbon has $a' \geq b'$. If $a' = b'$, then the different set ($a > b$) has precedence over the equal set ($a' = b'$). If $a' > b'$ and $a > a'$, then the different set ($a > b$) has precedence over the other set ($a' > b'$). These results are summarized to give the priority sequence $(a > b) \gg (a' \geq b')$. If the two sets, (a and b) and (a′ and b′), are identical with each other, the two possibilities should be examined, where either one is presumed to have precedence over the other.

As examples of the application of Rule 1, let us consider the promolecules shown in Fig. 4a. The promolecule **7** has a set of proligands A, B, X, and Y, the priority sequence is presumed to be $(A > X) \gg (B > Y)$. Hence, the label R_a is assigned to **7** by referring to the diagram **29** shown in Fig. 11. Similarly, the label S_a is assigned to its *RS*-diastereomer **13** (= $\overline{\mathbf{7}}$) by referring to the diagram **30** shown in Fig. 11. Thus, a pair of *RS*-diastereomers (**7** and **13**) is characterized by a pair of opposite labels R_a and S_a. In a parallel way, another pair of *RS*-diastereomers, $\overline{\mathbf{7}}$ and $\overline{\mathbf{13}}$ (= **7**), are characterized by a pair of opposite labels S_a and R_a.

[Rule 1] (The *RS*-Stereogenicity Rule for Three-Membered Heterocycles) Suppose that four proligands of an *RS*-stereogenic promolecule (a type-I, type-III, or type-V promolecule derived from an oxirane skeleton etc.) has the order of precedence represented by $(a > b) \gg (a' \geq b')$. Let us consider the vertical axis which runs through across the midpoint of the C—C bond and the hetero atom, as shown in Fig. 11. The path of the sequence of the higher proligands is determined to be a → b → opposite C-atom (with a′ and b′) around the vertical axis. The path of the sequence is examined whether it turns to right (clockwise) or left (anti-clockwise). According to this examination, the *RS*-stereogenic promolecule is assigned the *RS*-stereogenic label R_a (Rectus, right) or S_a (Sinister, left), or if chirality-unfaithful, r_a or s_a. If the two sets, (a and b) and (a′ and b′), are identical with each other, the two possibilities should be examined by presuming $(a > b) \gg (a' > b')$ or $(a' > b') \gg (a > b)$ tentatively: First, if they give an identical descriptor, this is adopted; second, if they give opposite descriptors, this is abandoned (type II or type IV).

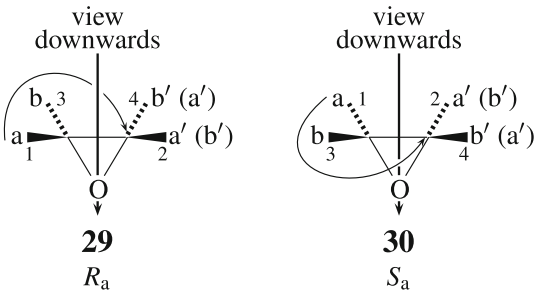

Fig. 11 R_a/S_a-Stereodescriptors assigned to a pair of *RS*-diastereomers according to the *RS*-stereogenicity rule, where the priority sequence is presumed to be $(a > b) \gg (a' \geq b')$. The path of the sequence of the higher proligands is determined to be a → b → opposite C-atom (with a′ and b′) around the vertical axis which runs through across the midpoint of the C—C bond and the oxygen atom

The promolecules **8** etc. shown in Fig. 4b are treated in a similar way, where a pair of *RS*-diastereomers (**8**/**14** or $\overline{\mathbf{8}}/\overline{\mathbf{14}}$) is characterized by a pair of opposite labels (R_a/S_a or S_a/R_a).

As one of general properties of type-I stereoisograms, a pair of labels R_a/S_a can be interpreted to be given to a pair of enantiomers $\mathbf{7}/\overline{\mathbf{7}}$ (or $\mathbf{8}/\overline{\mathbf{8}}$). However, this interpretation should be reexamined in terms of chirality faithfulness (cf. Sect. 6).

3.2 Specification of geometrical configurations

The next target is to develop a system of notation for differentiating geometrical configuration between stereoisomeric three-membered heterocycles, e.g., between **7** and **8**. This differentiation is akin to the *cis/trans*-isomerism of double bonds, so that the system of assigning *E/Z*-descriptors to double bonds [27–29] can be extended to develop such a system of notation for specifying geometrical configurations of three-membered heterocycles.

The practices for determining the order of precedence in the CIP system [1–3] are applied to the four proligands of an oxirane promolecule, where the set of two proligands (a and b) on one carbon has the order of precedence a > b and the set of two proligands on the other carbon has the order of precedence a′ > b′. Then the priority sequence represented by (a > b):(a′ > b′) is examined with respect

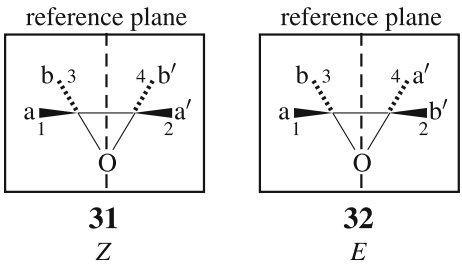

31 *Z* **32** *E*

Fig. 12 *Z/E*-Stereodescriptors assigned to a pair of stereoisomers according to Rule 2, where the priority sequence is presumed to be (a > b):(a′ > b′). The reference plane is selected to contain the three-membered ring

to the reference plane which contains the ring of the three-membered heterocycle (Fig. 12).

[Rule 2] (Assigning *E/Z*-Descriptors to Three-Membered Heterocycles) Suppose that four proligands of a three-membered heterocycle has the order of precedence represented by (a > b):(a′ > b′), where the higher set of proligands a and a′ is selected to be compared. If the proligands a and a′ are on the same side of the reference plane, an italic capital letter *Z* (Zusammen) is used (**31** in Fig. 12). If the proligands a and a′ are on opposite sides, an italic capital letter *E* (Entgegen) is used (**32** in Fig. 12).

As examples of the application of Rule 2, let us consider the promolecules shown in Fig. 6. The promolecule **7** has the priority sequence (A > X):(B > Y). Because the proligands A and B of the higher set are on the same side of the reference plane, a *Z*-descriptor is assigned to **7**. Each of the promolecules collected in the left stereoisogram of Fig. 6 is characterized by *Z*-descriptor in a similar way.

On the other hand, the promolecule **8**′ (= **8**) has the priority sequence (A > X):(B > Y), and is characterized by an *E*-descriptor, because the proligands A and B of the higher set are on opposite sides of the reference plane. Each of the promolecules collected in the right stereoisogram of Fig. 6 is characterized by an *E*-descriptor in a similar way.

By taking account of the multiple stereoisogram represented by Fig. 6, a pair of *Z/E*-descriptors is regarded as being assigned to a pair of *m*-diastereomeric stereoisograms (the left and right stereoisograms of Fig. 6) or as being assigned to a pair of *ortho*-diastereomeric promolecules (**7**/**8**′ etc. contained in the multiple stereoisogram). The renumbering of locants in **8**′ generates **8**, so that a pair of **7**/**8**′ corresponds to a pair of **7/8** contained in the two stereoisograms listed in Fig. 4. Hence, the pair of *Z/E*-descriptors assigned to the pair of **7/8**′ can be regarded as being assigned to a pair of **7/8**, if the locant numbers are not taken into consideration.

3.3 Specification of isoskeletomers

Because the proligand-promolecule model is adopted in this article, isoskeletomers are separated from isomers. By using a substitution function for generating a promolecule from the oxirane skeleton **5**, the isoskeletal group (Fig. 7) brings about promolecules in the form of a multiple stereoisogram set. The resulting promolecules are examined with respect to the assignability of R_a/S_a-descriptors as well as of *Z/E*-descriptors.

For example, the substitution function f_1 (Eq. 5) is applied to Fig. 7 so as to generate the multiple stereoisogram set shown in Fig. 8. The two stereoisograms at the top row of Fig. 8 have been already examined as two separate stereoisograms (Fig. 4a, b) under the *RS*-stereoisomeric group $\mathbf{C}_{2v\tilde{\sigma}\hat{I}}$ or as a multiple stereoisogram (Fig. 6) under the stereoisomeric group $\widetilde{\mathbf{C}}_{2v\tilde{\sigma}\hat{I}}$.

The two stereoisograms at the middle row of Fig. 8 can be examined in a similar way. The four proligands A, B, X, and Y of the promolecule **9** have the priority sequence (A > B) ≫ (X > Y) for Rule 1 as well as the the priority sequence (A > B):(X > Y) for Rule 2, so that the promolecule **9** is chracterized by R_a and *Z*. The promolecule **25** which is the *RS*-diastereomer of **9** has S_a and *Z*. The pair of R_a/S_a-stereodescriptors assigned to a pair of *RS*-diastereomers **9/25** can be interpreted to be given to a pair of enantiomers **9/$\overline{\mathbf{9}}$** because of the chirality faithfulness inherent in a type-I stereoisogram (cf. Sect. 6).

Similarly, the priority sequence (A > B) ≫ (X > Y) for Rule 1 and the priority sequence (A > B):(X > Y) for Rule 2 are given to the promolecule **10** and its *RS*-diastereomer **26**. They indicate, on the other hand, that R_a and *E* are assigned to **10**, while S_a and *E* are assigned to **26**. The pair of R_a/S_a-stereodescriptors assigned to a pair of *RS*-diastereomers **10/26** can be interpreted to be given to a pair of enantiomers **10/$\overline{\mathbf{10}}$** because of the chirality faithfulness of a type-I stereoisogram (cf. Sect. 6).

A pair of *Z/E*-descriptors is given to a pair of *ortho*-diastereomers or a pair of *m*-diastereomeric stereoisograms. Thus, a pair of *Z/E*-descriptors is given a pair of **9** and **10**, which are in an *ortho*-diastereomeric relationship. Such a pair of *Z/E*-descriptors can be also considered to give a pair of the stereoisogram for **9** and that of **10**, which are in a *m*-diastereomeric relationship.

The two stereoisograms at the bottom row of Fig. 8 can be examined in a similar way by using the priority sequence (A > Y) ≫ (B > X) for Rule 1 as well as the the priority sequence (A > Y):(B > X) for Rule 2 The assignments are attached at the head of each promolecule contained in each stereoisogram, e.g., R_a and *Z* are assigned to **11**; and R_a and *E* are assigned to **12**.

Finally, each of the stereoisograms contained in the multiple stereoisogram set for ABXY (type I–I/I–I/I–I for $[\theta]_{10}$) can be characterized by R_a/S_a-stereodescriptors. To show the assignability of R_a/S_a, the symbol Y–Y/Y–Y/Y–Y is shown at the intersection between the $[\theta]_{10}$-row and the assignability-column in Table 1, where the letter Y denotes 'Yes'.

Each of the multiple stereoisograms contained in the multiple stereoisogram set for ABXY (type I–I/I–I/I–I for $[\theta]_{10}$) can be characterized by *Z/E*-descriptors. Hence, the symbol Y/Y/Y is shown at the intersection between the $[\theta]_{10}$-row and the (assignability-of-*Z/E*)-column in Table 1, where the letter Y denotes 'Yes'.

4 Examples for non-degenerate cases

4.1 Promolecules of ABXp

Let us consider promolecules of the composition ABXp (the partition $[\theta]_{11}$ of Part I), where A, B, and X are achiral proligands and p is a chiral proligand in isolation.

There are six promolecules shown in Fig. 13 under the action of the *RS*-stereoisomeric group $\mathbf{C}_{2v\widetilde{\sigma}\widehat{I}}$, as reported in Part I of this series. Each of these promolecules belongs to a type-III stereoisogram.

To discuss the total features of isomerism, a substitution function:

$$f_7 : f_7(1) = \mathrm{A},\ f_7(2) = \mathrm{B},\ f_7(3) = \mathrm{X},\ f_7(4) = \mathrm{p} \tag{16}$$

is applied to Fig. 7, where the value $f_7(\overline{4}) = \overline{\mathrm{p}}$ is used to denote an mirror-image proligand of p. Thereby, a multiple stereoisogram set of type III–III/III–III/III–III is generated, as shown in Fig. 14.

The types of component stereoisograms are determined by using the flowchart shown in Fig. 9. Thereby, the starting set:

$$\left\{ \frac{\mathbf{33}\,\mathbf{39}}{\mathbf{33}\,\mathbf{39}}\ \frac{\mathbf{34}\,\mathbf{40}}{\mathbf{34}\,\mathbf{40}}\ \frac{\mathbf{35}\,\mathbf{41}}{\mathbf{35}\,\mathbf{41}}\ \frac{\mathbf{36}\,\mathbf{42}}{\mathbf{36}\,\mathbf{42}}\ \frac{\mathbf{37}\,\mathbf{43}}{\mathbf{37}\,\mathbf{43}}\ \frac{\mathbf{38}\,\mathbf{44}}{\mathbf{38}\,\mathbf{44}} \right\} \tag{17}$$

is divided into a final set:

$$\left\{ \left\langle \left(\frac{\mathbf{33}\,\mathbf{39}}{\mathbf{33}\,\mathbf{39}} \right) \left(\frac{\mathbf{34}\,\mathbf{40}}{\mathbf{34}\,\mathbf{40}} \right) \right\rangle \left\langle \left(\frac{\mathbf{35}\,\mathbf{41}}{\mathbf{35}\,\mathbf{41}} \right) \left(\frac{\mathbf{36}\,\mathbf{42}}{\mathbf{36}\,\mathbf{42}} \right) \right\rangle \left\langle \left(\frac{\mathbf{37}\,\mathbf{43}}{\mathbf{37}\,\mathbf{43}} \right) \left(\frac{\mathbf{38}\,\mathbf{44}}{\mathbf{38}\,\mathbf{44}} \right) \right\rangle \right\}, \tag{18}$$

where each stereoisogram in a pair of parentheses is determined to be type III so that each stereoisogram set in a pair of angle brackets is denoted by the symbol III–III. Hence, the multiple stereoisogram set of Fig. 14 is denoted by the symbol III–III/III–III/III–III, as listed in the $[\theta]_{11}$-row of Table 1. The resulting promolecules are labelled by $R_\mathrm{a}/S_\mathrm{a}$-stereodescriptors and *Z*/*E*-descriptors, as attached at the head of each promolecule in Fig. 14.

Each of the stereoisograms contained in the multiple stereoisogram set for ABXp (type III–III/III–III/III–III for $[\theta]_{11}$) can be characterized by $R_\mathrm{a}/S_\mathrm{a}$-stereodescriptors. A pair of $R_\mathrm{a}/S_\mathrm{a}$-stereodescriptors is given to a pair of *RS*-diastereomers appearing along the horizontal alignment of each stereoisogram. For example, compare the label R_a, *Z* for **33** with the label S_a, *Z* for **39** in the first stereoisogram of Fig. 14, where the stereodescriptors R_a and S_a are determined by using a common priority sequence (A > X) ≫ (B > p) for Rule 1. To show the assignability of $R_\mathrm{a}/S_\mathrm{a}$, the symbol Y–Y/Y–Y/Y–Y is shown at the intersection between the $[\theta]_{11}$-row and the assignability-column in Table 1, where the letter Y denotes 'Yes' which means that a pair of $R_\mathrm{a}/S_\mathrm{a}$ can be assigned.

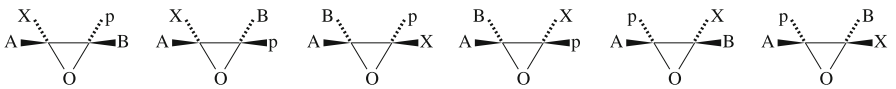

Fig. 13 Six oxiranes with the composition ABXp (the partition $[\theta]_{11}$), each of which is a representative of a quadruplet contained in a type-III stereoisogram. The symbols A, B, and X denote proligands which are achiral in isolation and the symbol p denotes a chiral proligand in isolation. Each of the six oxiranes belongs to the *RS*-stereoisomeric group $\mathbf{C}_1$, the point group $\mathbf{C}_1$, and the *RS*-permutation group $\mathbf{C}_1$. For the partition $[\theta]_{11}$, see Part I

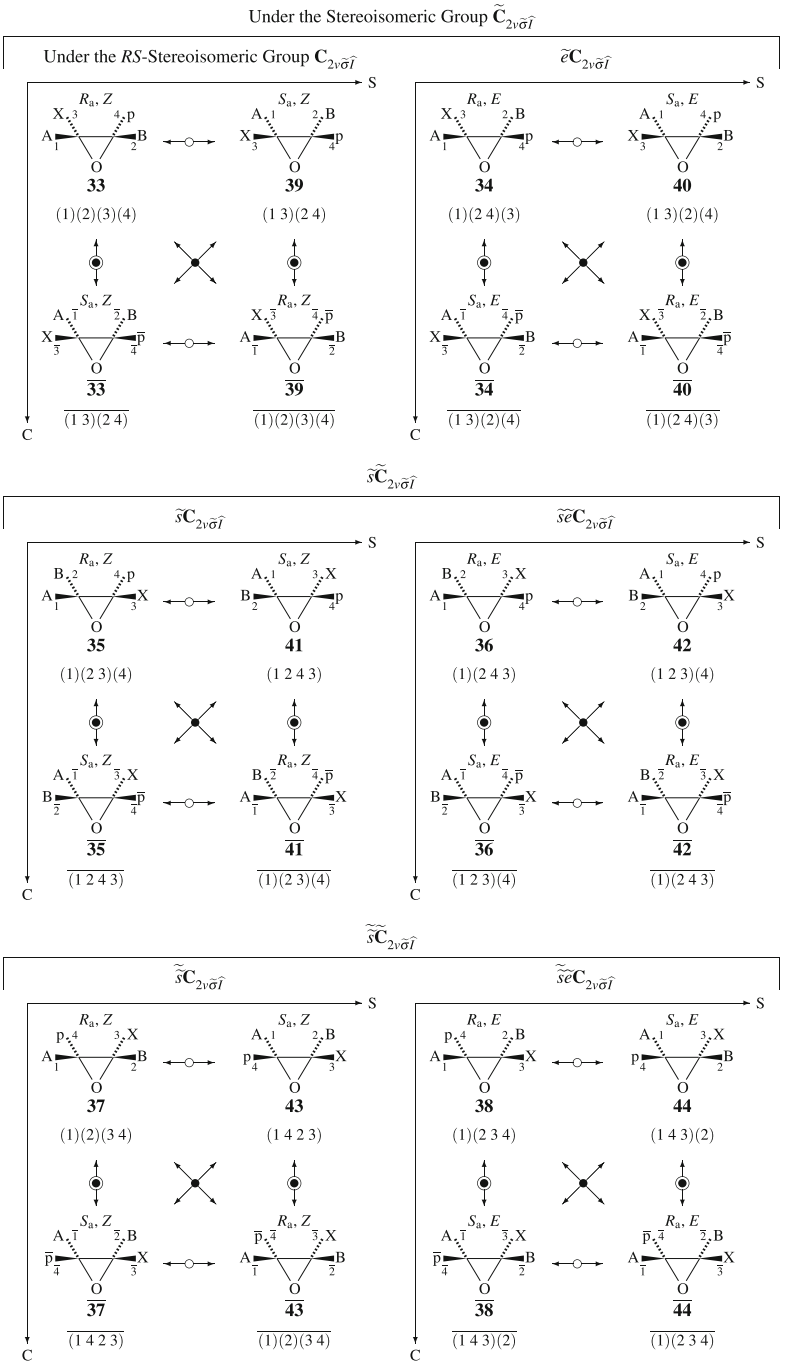

$$f_7 : f_7(1) = \mathrm{A}, f_7(2) = \mathrm{B}, f_7(3) = \mathrm{X}, f_7(4) = \mathrm{p}$$

Fig. 14 Multiple stereoisogram set of type III–III/III–III/III–III derived from the oxirane skeleton **5**, where the substitution function f_7 is applied to Fig. 7. Note that the proligands A, B, and X are achiral in isolation, while a pair of p/$\overline{\mathrm{p}}$ represents a pair of chiral proligands with opposite chirality sense

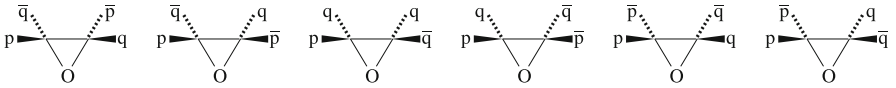

Fig. 15 Six oxiranes with the composition $p\bar{p}q\bar{q}$ (the partition $[\theta]_{28}$), each of which is a representative of a quadruplet contained in a type-I or type-V stereoisogram. Each of the six oxiranes belongs to an *RS*-stereoisomeric group ($\mathbf{C}_{\widehat{\sigma}}$, $\mathbf{C}_s$, or $\mathbf{C}'_s$), a point group ($\mathbf{C}_1$, $\mathbf{C}_s$, or $\mathbf{C}'_s$), and an *RS*-permutation group ($\mathbf{C}_1$) attached below each promolecule. For the partition $[\theta]_{28}$, see Part I

Each of the multiple stereoisograms contained in the multiple stereoisogram set for ABXp (type III–III/III–III/III–III for $[\theta]_{11}$) can be characterized by *Z/E*-descriptors. A pair of *Z/E*-descriptors is given to a pair of *m*-diastereomeric stereoisograms (in a multiple stereoisogram) or to a pair of *ortho*-diastereomers appearing at the corresponding quarters in the multiple stereoisogram. For example, compare the label R_a, *Z* for **33** (in the first stereoisogram of Fig. 14) with the label R_a, *E* for **34** (in the second stereoisogram of Fig. 14), where the descriptors *Z* and *E* are determined by using a common priority sequence (A > X):(B > p) for Rule 2. The symbol Y/Y/Y is shown at the intersection between the $[\theta]_{11}$-row and the (assignability-of-*Z/E*)-column in Table 1, where the letter Y denotes 'Yes'.

The partitions $[\theta]_{14}$ (ABpq), $[\theta]_{18}$ (Ap$\bar{p}$q), $[\theta]_{19}$ (Apqr), $[\theta]_{29}$ (p$\bar{p}$qr), and $[\theta]_{30}$ (pqrs) are characterized by multiple stereoisogram sets of type III–III/III–III/III–III, so that the assignabilities of stereodescriptors are examined in a similar way, as collected in the corresponding rows of Table 1.

4.2 Promolecules of $p\bar{p}q\bar{q}$

Let us consider promolecules of the composition $p\bar{p}q\bar{q}$ (the partition $[\theta]_{28}$ of Part I), where a pair of lowercase letters p/$\bar{p}$ or q/$\bar{q}$ denotes a pair of a chiral proligand and its enantiomeric counterpart in isolation. As enumerated in Part I of this series, there are six promolecules shown in Fig. 15 under the action of the *RS*-stereoisomeric group $\mathbf{C}_{2v\widetilde{\sigma}\widehat{I}}$. The stereoisogram of each promolecule exhibits type-I or type-V.

To discuss the isomerism concerning **45**–**50**, the following substitution function is applied to Fig. 7:

$$f_8 : f_8(1) = \mathrm{p},\ f_8(2) = \bar{\mathrm{p}},\ f_8(3) = \mathrm{q},\ f_8(4) = \bar{\mathrm{q}}. \tag{19}$$

Thereby, a multiple stereoisogram set of type I–V/I–V/V–V is generated, as shown in Fig. 16. The types of component stereoisograms are determined by using the flowchart shown in Fig. 9. Thereby, the corresponding starting set is obtained by omitting inner congruence in each type-I or type-V stereoisogram as follows:

$$\left\{\frac{\mathbf{45}}{\mathbf{45}}\ \ \mathbf{46\ 52}\ \ \frac{\mathbf{47}}{\mathbf{47}}\ \ \mathbf{48\ 54}\ \ \mathbf{49\ 55}\ \ \mathbf{50\ 56}\right\}. \tag{20}$$

By using Fig. 9, this set is divided into a final set:

$$\left\{\left\langle\left(\frac{\mathbf{45}}{\mathbf{45}}\right)\,(\mathbf{46}\ \mathbf{52})\right\rangle\left\langle\left(\frac{\mathbf{47}}{\mathbf{47}}\right)\,(\mathbf{48}\ \mathbf{54})\right\rangle\langle(\mathbf{49}\ \mathbf{55})\,(\mathbf{50}\ \mathbf{56})\rangle\right\}, \tag{21}$$

where each stereoisogram in a pair of parentheses is determined to be type I or type V, so that the stereoisogram sets in a pair of angle brackets are respectively denoted by the symbols I–V, I–V, and V–V. Hence, the multiple stereoisogram set of Fig. 16 is denoted by the symbol I–V/I–V/V–V. The resulting promolecules are labelled by R_a/S_a-stereodescriptors and *Z/E*-descriptors, as attached at the head of each promolecule in Fig. 16.

A pair of R_a/S_a-stereodescriptors is given to a pair of *RS*-diastereomers appearing along the horizontal alignment of each stereoisogram.

1. As an example of a type-I case, compare the label R_a, *E* for **45** with the label S_a, *E* for **51** (= $\overline{\mathbf{45}}$) in the first stereoisogram of Fig. 16, where the stereodescriptors R_a and S_a are determined by using a common priority sequence $(p > \overline{q}) \gg (\overline{p} > q)$ for Rule 1. The assigned labels given originally to the pair of *RS*-diastereomers **45** and **51** can be interpreted to be given to a pair of enantiomers **45** and $\overline{\mathbf{45}}$ because of the congruence between **51** and $\overline{\mathbf{45}}$. Another pair of **47** and **53** (= $\overline{\mathbf{47}}$) in the third stereoisogram of Fig. 16 can be discussed in a similar way.
2. As an example of a type-V case, compare the label r_a, *Z* for **46** with the label s_a, *Z* for **52** in the second stereoisogram of Fig. 16, where the stereodescriptors r_a and s_a are determined by using a common priority sequence $(p > \overline{q}) \gg (\overline{p} > q)$ for Rule 1. The assigned labels are given to the pair of *RS*-diastereomers **46** and **52**, where there are no enantiomeric relationships because **46** and **52** are both achiral. The labels are shown by lowercase letters to emphasize chirality unfaithfulness (cf. Sect. 6). This case exhibits extended pseudoasymmetry discussed in a previous article [30]. In a similar way, another pair of *RS*-diastereomers **48** and **54** in the 4th stereoisogram of Fig. 16 exhibits extended pseudoasymmetry. See Sect. 6.4.
3. As another example of a type-V case, compare the label r_a, *Z* for **49** with the label s_a, *Z* for **55** in the 5th stereoisogram of Fig. 16, where the stereodescriptors r_a and s_a are determined by using a common priority sequence $(p > \overline{p}) \gg (\overline{q} > q)$ for Rule 1. The pseudoasymmetry of this case can be detected by the conventional methodology, as will be discussed in Part III of this series.

As a result, each of the stereoisograms contained in the multiple stereoisogram set for $p\overline{p}q\overline{q}$ (type I–V/I–V/V–V for $[\theta]_{28}$) can be characterized by R_a/S_a-stereodescriptors. This is summarized by the symbol Y–Y/Y–Y/Y–Y appearing in the $[\theta]_{28}$-row of Table 1, where the letter Y indicates the assignability of an R_a/S_a-stereodescriptor.

A pair of *Z/E*-descriptors is given to a pair of *m*-diastereomeric stereoisograms (in a multiple stereoisogram) or to a pair of *ortho*-diastereomers appearing at the corresponding quarters in the multiple stereoisogram. For example, compare the label R_a, *E* for **45** (in the first stereoisogram of Fig. 16) with the label r_a, *Z* for **46** (in the second stereoisogram of Fig. 16), where the descriptors *E* and *Z* are determined by using a common priority sequence $(p > \overline{q})$:$(\overline{p} > q)$ for Rule 2. This is summarized by the symbol Y/Y/Y appearing in the $[\theta]_{28}$-row of Table 1, where the letter Y indicates the assignability of a *Z/E*-descriptor.

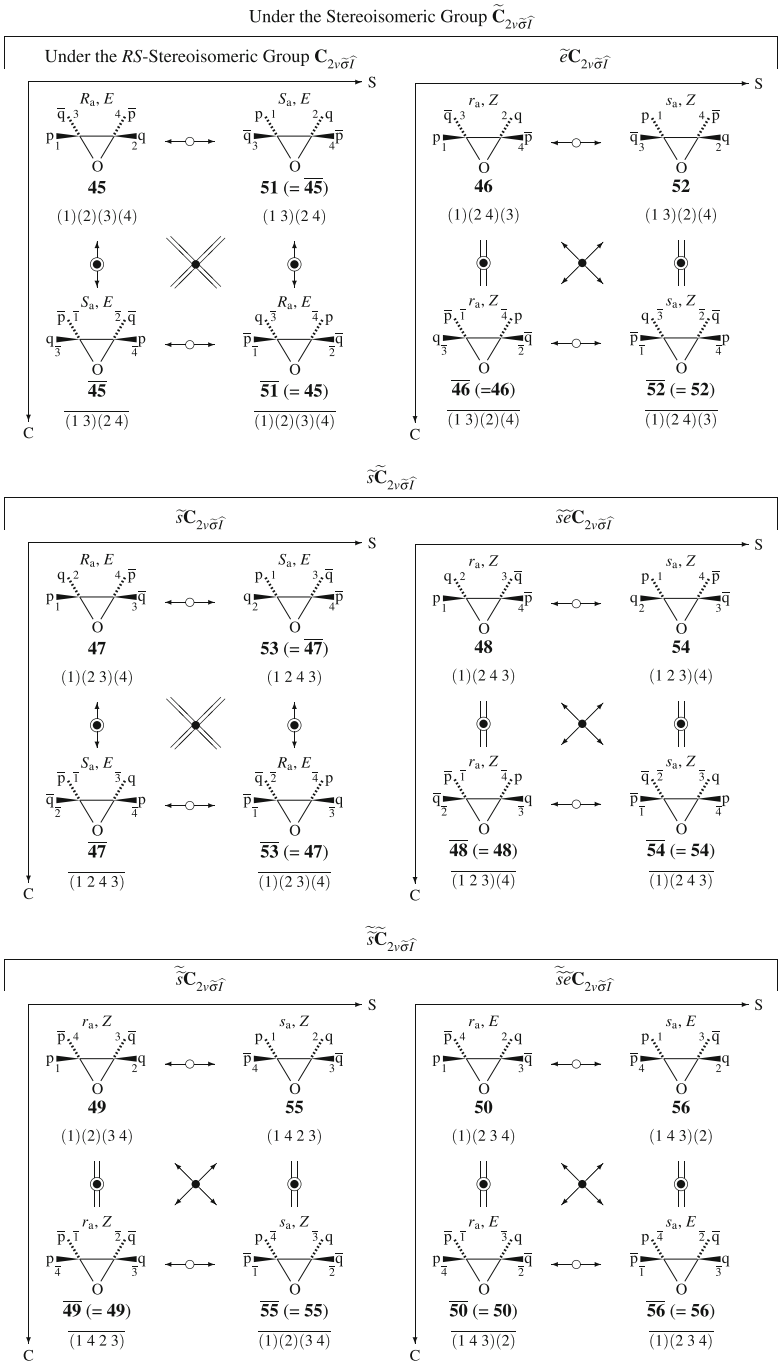

Fig. 16 Multiple stereoisogram set of type I–V/I–V/V–V derived from the oxirane skeleton **5**, where the substitution function f_8 is applied to Fig. 7. Note that a pair of p/$\overline{\mathrm{p}}$ and another pair of q/$\overline{\mathrm{q}}$ represent pairs of chiral proligands with opposite chirality senses. The priority sequence is presumed to be $\mathrm{p} > \overline{\mathrm{p}} > \mathrm{q} > \overline{\mathrm{q}}$

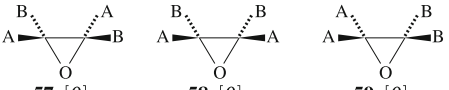

Fig. 17 Three oxiranes with the composition A^2B^2 (the partition $[\theta]_4$), each of which is a representative of a quadruplet contained in a type-I or type-IV stereoisogram. Each of the three oxiranes belongs to an *RS*-stereoisomeric group, a point group, and an *RS*-permutation group, as attached below each promolecule. For the partition $[\theta]_4$, see Part I

5 Examples for degenerate cases

5.1 Promolecules of A^2B^2

As enumerated in Part I of this series, there are three quadruplets of promolecules having the composition A^2B^2 (the partition $[\theta]_4$ of Part I) under the action of the *RS*-stereoisomeric group $\mathbf{C}_{2v\widetilde{\sigma}\widehat{I}}$, where the uppercase letters A and B denote achiral proligands in isolation. They are depicted in Fig. 17, where the stereoisogram of each promolecule exhibits type-I or type-IV.

A multiple stereoisogram set for **57**–**59** is generated by applying the following substitution function to Fig. 7:

$$f_9 : f_9(1) = \mathrm{A},\ f_9(2) = \mathrm{B},\ f_9(3) = \mathrm{B},\ f_9(4) = \mathrm{A} \tag{22}$$

As a result, the multiple stereoisogram set depicted in Fig. 18 exhibits degenerate nature as denoted by the symbol $(\mathrm{I–IV})^2/\mathrm{IV}^2$. The types of component stereoisograms in the symbol $(\mathrm{I–IV})^2/\mathrm{IV}^2$ are determined by using the flowchart shown in Fig. 9.

Thereby, the corresponding starting set is obtained by omitting inner congruence in each type-I or type-IV stereoisogram as follows:

$$\left\{\frac{\mathbf{57}}{\mathbf{57}}\quad \mathbf{58}\quad \mathbf{59}\right\}. \tag{23}$$

By using Fig. 9, this set is divided into a final set:

$$\left\{\left\langle\left(\frac{\mathbf{57}}{\mathbf{57}}\right)(\mathbf{58})\right\rangle\langle(\mathbf{59})\rangle\right\}, \tag{24}$$

where each stereoisogram in a pair of parentheses is determined to be type I or type IV. The multiple stereoisogram in the first pair of angle brackets of Eq. 24, which is denoted by the symbol I–IV, appears in the top row of the multiple stereoisogram set (Fig. 18). The middle row of Fig. 18 is omitted because it is congruent to the top row. This congruence is denoted by the symbol $(\mathrm{I–IV})^2$. The multiple stereoisogram in the second pair of angle brackets of Eq. 24 consists of one pair of parentheses (type IV) containing an achiral promolecule **59**, so that the third row of Fig. 18 degenerates, as shown by the symbol IV^2. Hence, the total feature of the multiple stereoisogram set (Fig. 18) is denoted by the symbol $(\mathrm{I–IV})^2/\mathrm{IV}^2$.

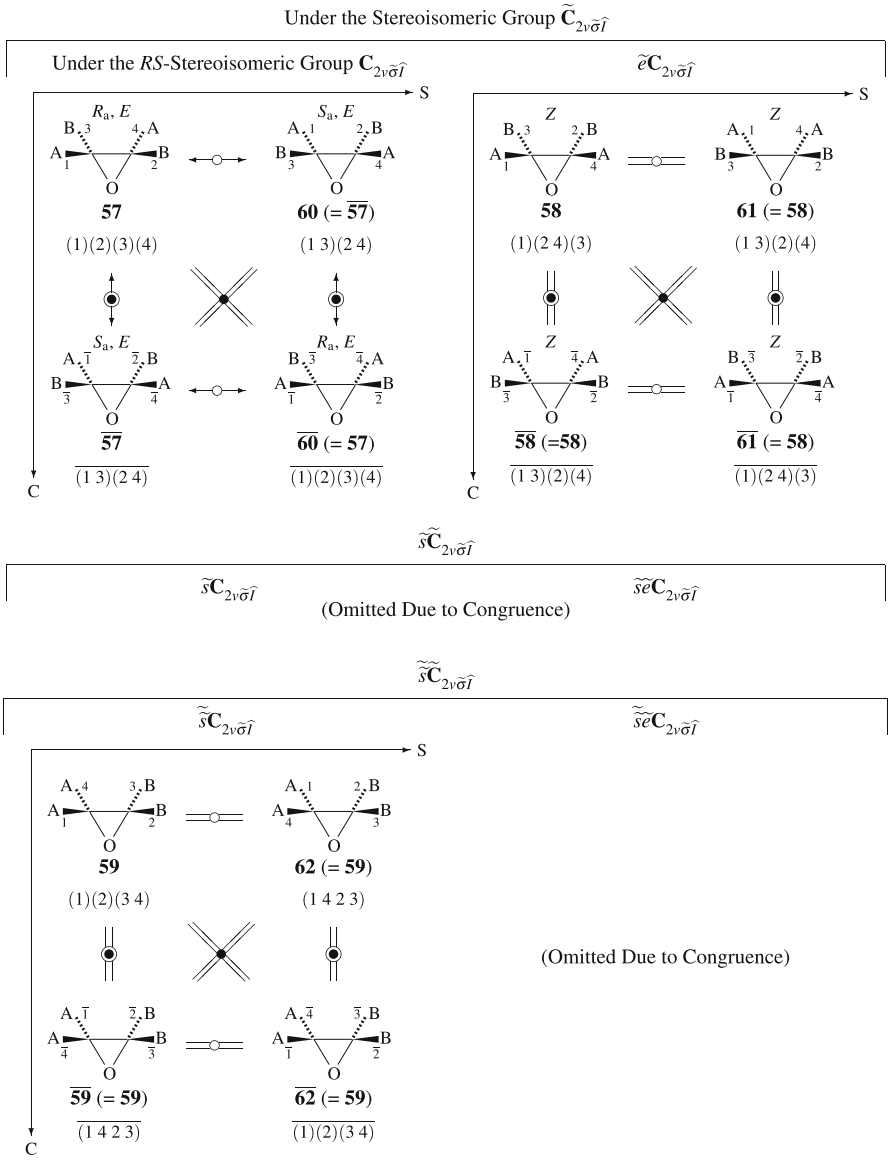

Fig. 18 Multiple stereoisogram set of type $(\mathrm{I–IV})^2/\mathrm{IV}^2$ derived from the oxirane skeleton **5**, where the substitution function f_9 is applied to Fig. 7. Note that the uppercase letters A and B represent achiral proligands in isolation, where the priority sequence is presumed to be A > B

A pair of *RS*-diastereomers **57/60** is labelled by a pair of R_a/S_a-stereodescriptors. Because of type I, the pair of R_a/S_a-stereodescriptors is allowed to be applied to a pair of enantiomers **57/$\overline{\mathbf{57}}$**. The stereodescriptors R_a and S_a are determined by using

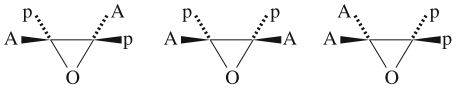

Fig. 19 Three oxiranes with the composition A^2p^2 (the partition $[\theta]_5$), each of which is a representative of a quadruplet contained in a type-III or type-II stereoisogram. Each of the three oxiranes belongs to an *RS*-stereoisomeric group, a point group, and an *RS*-permutation group, as attached below each promolecule. For the partition $[\theta]_5$, see Part I

a common priority sequence (A > B) ≫ (A > B) for Rule 1. Because of type IV, the promolecule **58** exhibits no assignability of R_a/S_a-stereodescriptors, so that the symbol Y–N is assigned. Totally, by adding the data N for **59**, the symbol Y–N/N is determined to characterize the multiple stereoisogram set of type $(\text{I–IV})^2/\text{IV}^2$, as listed in the $[\theta]_4$-row of Table 1.

A pair of *Z/E*-descriptors is given to a pair of *m*-diastereomeric stereoisograms (in a multiple stereoisogram) or to a pair of *ortho*-diastereomers (i.e., **57**/**58**). Compare the label R_a, *E* for **57** (in the first stereoisogram of Fig. 18) with the label *Z* for **58** (in the second stereoisogram of Fig. 18), where the descriptors *E* and *Z* are determined by using a common priority sequence (A > B):(A > B) for Rule 2. The label N in the symbol Y/N listed in the $[\theta]_4$-row of Table 1 means the lack of *Z/E*-descriptors for **59** because of the absence of *cis/trans*-isomerism.

5.2 Promolecules of A^2p^2

As enumerated in Part I of this series, there are three quadruplets of promolecules having the composition A^2p^2 (the partition $[\theta]_5$ of Part I) under the action of the *RS*-stereoisomeric group $\mathbf{C}_{2v\widetilde{\sigma}\widehat{I}}$, where the uppercase letter A denotes an achiral proligand and the lowercase letter p denotes a chiral proligand in isolation. They are depicted in Fig. 19, where the stereoisogram of each promolecule exhibits type-III or type-II.

To discuss the total features of isomerism, a substitution function:

$$f_{10} : f_{10}(1) = \text{A},\ f_{10}(2) = \text{p},\ f_{10}(3) = \text{p},\ f_{10}(4) = \text{A} \tag{25}$$

is applied to Fig. 7, where the value $f_{10}(\overline{2}) = \overline{\text{p}}$ is used to denote an mirror-image proligand of p. Thereby, a multiple stereoisogram set of type $(\text{III–II})^2/\text{II}^2$ is generated, as shown in Fig. 20. The types of component stereoisograms appearing in the symbol $(\text{III–II})^2/\text{II}^2$ are determined by using the flowchart shown in Fig. 9. Thereby, the starting set:

$$\left\{ \begin{matrix} \mathbf{63}\,\mathbf{66} \\ \mathbf{63}\,\mathbf{66} \end{matrix} \quad \begin{matrix} \mathbf{64} \\ \mathbf{64} \end{matrix} \quad \begin{matrix} \mathbf{65} \\ \mathbf{65} \end{matrix} \right\}, \tag{26}$$

is divided into a final set:

$$\left\{ \left\langle \left(\begin{matrix} \mathbf{63}\,\mathbf{66} \\ \mathbf{63}\,\mathbf{66} \end{matrix} \right) \left(\begin{matrix} \mathbf{64} \\ \mathbf{64} \end{matrix} \right) \right\rangle \left\langle \left(\begin{matrix} \mathbf{65} \\ \mathbf{65} \end{matrix} \right) \right\rangle \right\}. \tag{27}$$

where each stereoisogram in a pair of parentheses is determined to be type III or type II.

The multiple stereoisogram in the first pair of angle brackets of Eq. 27, which is denoted by the symbol III–II, appears in the top row of the multiple stereoisogram set (Fig. 20). The middle row of Fig. 20 is omitted because it is congruent to the top row. This congruence is denoted by the symbol $(\text{III–II})^2$. The multiple stereoisogram in the second pair of angle brackets of Eq. 27 consists of one pair of parentheses (type II) so that the third row of Fig. 20 degenerates, as shown by the symbol II^2. Hence, the total feature of the multiple stereoisogram set (Fig. 20) is denoted by the symbol $(\text{III–II})^2/\text{II}^2$, as listed in the $[\theta]_5$-row of Table 1.

Because of type III, a pair of *RS*-diastereomers **63/66** is labelled by a pair of stereodescriptors R_a and S_a by using the priority sequence $(\text{A} > \text{p}) \gg (\text{A} > \text{p})$; and another pair of *RS*-diastereomers $\overline{\mathbf{63}}/\overline{\mathbf{66}}$ is labelled by a pair of stereodescriptors S_a and R_a by using the priority sequence $(\text{A} > \overline{\text{p}}) \gg (\text{A} > \overline{\text{p}})$. The stereodescriptors R_a and S_a assigned originally to a pair of *RS*-diastereomers **63/66** can be interpreted to give a pair of enantiomers $\mathbf{63}/\overline{\mathbf{63}}$ because of chirality faithfulness, although the priority sequence $(\text{A} > \text{p}) \gg (\text{A} > \text{p})$ for **63** is different from $(\text{A} > \overline{\text{p}}) \gg (\text{A} > \overline{\text{p}})$ for $\overline{\mathbf{63}}$.

The promolecule **64** is a representative of a type-II stereoisogram as shown in the right-side of the top row of Fig. 20. Because of type II, the promolecule exhibits no assignability of R_a/S_a-stereodescriptors. This case is an example of the second case in which (a and b) and (a′ and b′) are identical with each other, as described in Rule 1. It follows that no assignability of R_a/S_a-stereodescriptors do not linked with the chirality or the presence of a pair of enantiomers of $\mathbf{64}/\overline{\mathbf{64}}$.

A pair of *Z/E*-descriptors is given to a pair of *m*-diastereomeric stereoisograms (in a multiple stereoisogram) or to a pair of *ortho*-diastereomers (i.e., **63/64**), i.e., *E* for **63** etc. and *Z* for **64** etc. by using the priority sequence $(\text{A} > \text{p}):(\text{A} > \text{p})$ for Rule 2.

The remaining promolecule **65** is a representative of a type-II stereoisogram as shown in the bottom row of Fig. 20 and exhibits no assignabilities of R_a/S_a-stereodescriptors and of *Z/E*-descriptors.

The partition $[\theta]_{25}(\text{p}^2\text{q}^2)$ is characterized by a multiple stereoisogram set of type $(\text{III–II})^2/\text{II}^2$, so that the assignabilities of stereodescriptors are examined in a similar way to $[\theta]_5$ (A^2q^2), as collected in the corresponding row of Table 1.

5.3 Promolecules of A^2BX

As enumerated in Part I of this series, there are three quadruplets of promolecules having the composition A^2BX (the partition $[\theta]_6$ of Part I) under the action of the *RS*-stereoisomeric group $\mathbf{C}_{2v\widetilde{\sigma}\widehat{I}}$, where the uppercase letters A, B, and X denote achiral proligands in isolation. They are depicted in Fig. 21, where the stereoisogram of each promolecule exhibits type-I.

To discuss the total features of isomerism, a substitution function:

$$f_{11} : f_{11}(1) = \text{A}, f_{11}(2) = \text{A}, f_{11}(3) = \text{B}, f_{11}(4) = \text{X} \tag{28}$$

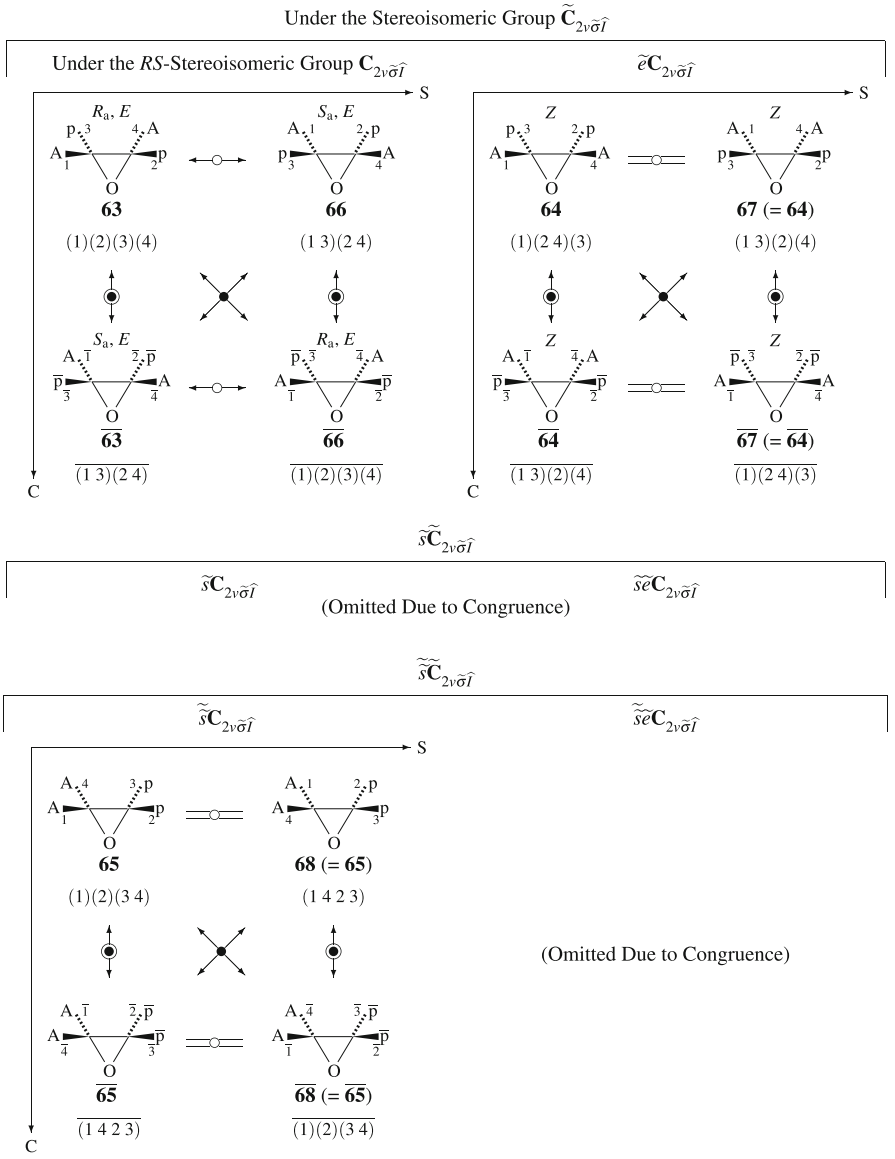

$$f_{10} : f_{10}(1) = \mathrm{A}, f_{10}(2) = \mathrm{p}, f_{10}(3) = \mathrm{p}, f_{10}(4) = \mathrm{A}$$

Fig. 20 Multiple stereoisogram set of type $(\mathrm{III–II})^2/\mathrm{II}^2$ derived from the oxirane skeleton **5**, where the substitution function f_{10} is applied to Fig. 7. Note that the uppercase letter A represents an achiral proligand in isolation and the lowercase letter p represents a chiral proligand in isolation, where the priority sequence is presumed to be A > p

is applied to Fig. 7. Thereby, a multiple stereoisogram set of type $(\mathrm{I–I})^2/\mathrm{I}^2$ is generated, as shown in Fig. 22.

The types of component stereoisograms appearing in the symbol $(\mathrm{I–I})^2/\mathrm{I}^2$ are determined by using the flowchart shown in Fig. 9. Thereby, the starting set:

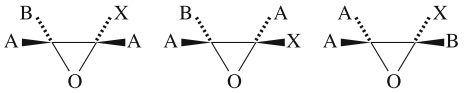

69, $[\theta]_6$ **70**, $[\theta]_6$ **71**, $[\theta]_6$

$\mathbf{C}_{\widehat{I}}, \mathbf{C}_1, \mathbf{C}_1, \mathrm{I}$ $\mathbf{C}_{\widehat{I}}, \mathbf{C}_1, \mathbf{C}_1, \mathrm{I}$ $\mathbf{C}_{\widehat{I}}, \mathbf{C}_1, \mathbf{C}_1, \mathrm{I}$

Fig. 21 Three oxiranes with the composition A^2BX (the partition $[\theta]_6$), each of which is a representative of a quadruplet contained in a type-I stereoisogram. Each of the three oxiranes belongs to an *RS*-stereoisomeric group, a point group, and an *RS*-permutation group, as attached below each promolecule. For the partition $[\theta]_6$, see Part I

$$\left\{\frac{\mathbf{69}}{\mathbf{69}} \quad \frac{\mathbf{70}}{\mathbf{70}} \quad \frac{\mathbf{71}}{\mathbf{71}}\right\}. \tag{29}$$

is divided into a final set:

$$\left\{\left\langle\left(\frac{\mathbf{69}}{\mathbf{69}}\right)\left(\frac{\mathbf{70}}{\mathbf{70}}\right)\right\rangle\left\langle\left(\frac{\mathbf{71}}{\mathbf{71}}\right)\right\rangle\right\}. \tag{30}$$

where each stereoisogram in a pair of parentheses is determined to be type I.

The multiple stereoisogram in the first pair of angle brackets of Eq. 30, which is denoted by the symbol I–I, appears in the top row of the multiple stereoisogram set (Fig. 22). The middle row of Fig. 22 is omitted because it is congruent to the top row. This congruence is denoted by the symbol $(\mathrm{I–I})^2$. The multiple stereoisogram in the second pair of angle brackets of Eq. 30 consists of one pair of parentheses (type I) so that the third row of Fig. 22 degenerates, as shown by the symbol I^2. Hence, the total feature of the multiple stereoisogram set (Fig. 22) is denoted by the symbol $(\mathrm{I–I})^2/\mathrm{I}^2$, as listed in the $[\theta]_6$-row of Table 1.

A pair of *RS*-diastereomers **69/72** is labelled by a pair of stereodescriptors R_a and S_a by using the priority sequence $(\mathrm{A} > \mathrm{B}) \gg (\mathrm{A} > \mathrm{X})$; and another pair of *RS*-diastereomers $\overline{\mathbf{69}}/\overline{\mathbf{72}}$ is labelled by a pair of stereodescriptors S_a and R_a by using the priority sequence $(\mathrm{A} > \mathrm{B}) \gg (\mathrm{A} > \mathrm{X})$. Because the *RS*-diastereomeric relationships coalesce with the enantiomeric relationships in a type-I stereoisogram, the stereodescriptors R_a and S_a assigned originally to a pair of *RS*-diastereomers **69/72** can be interpreted to give a pair of enantiomers $\mathbf{69}/\overline{\mathbf{69}}$. Similarly, the promolecule **70** exhibits the assignability of $R_\mathrm{a}/S_\mathrm{a}$-stereodescriptors by using $(\mathrm{A} > \mathrm{B}) \gg (\mathrm{A} > \mathrm{X})$ in the application of Rule 1.

On the other hand, the priority sequence $(\mathrm{B} > \mathrm{X}) \gg (\mathrm{A} = \mathrm{A})$ for the application of Rule 1 to the promolecule **71** stems from the condition that the different set $(\mathrm{a} > \mathrm{b})$ has precedence over the equal set $(\mathrm{a}' = \mathrm{b}')$. Thereby a pair of *RS*-diastereomers **71/74** is labelled by a pair of stereodescriptors $S_\mathrm{a}/R_\mathrm{a}$, which is interpreted to give to a pair of enantiomers $\mathbf{71}/\overline{\mathbf{71}}$.

A pair of *Z/E*-descriptors is given to a pair of *m*-diastereomeric stereoisograms (in a multiple stereoisogram) or to a pair of *ortho*-diastereomers (i.e., **69/70**), i.e., *Z* for **69** etc. and *E* for **70** etc. by using the priority sequence $(\mathrm{A} > \mathrm{B})$:$(\mathrm{A} > \mathrm{X})$ for Rule 2.

The promolecule **71** exhibits no assignability of of *Z/E*-descriptors, while it can be labelled by an S_a-stereodescriptor.

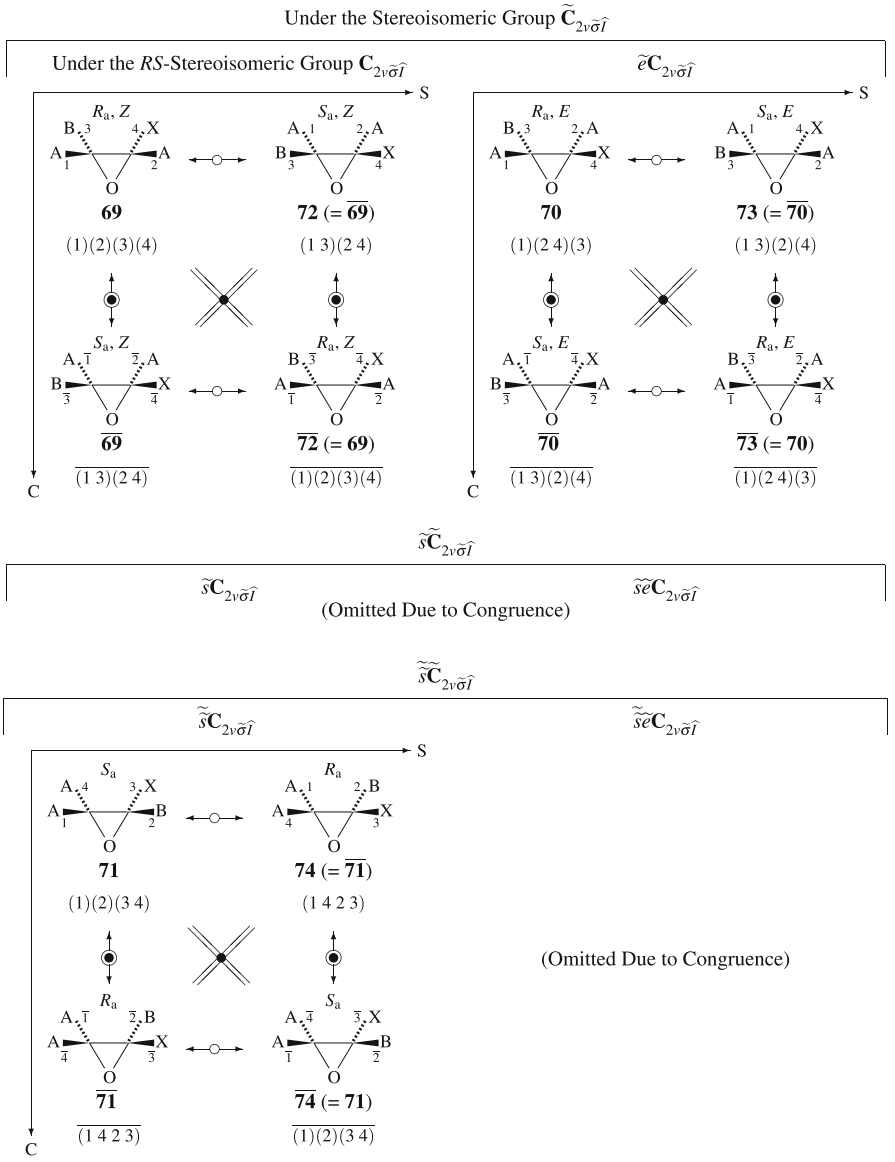

$$f_{11} : f_{11}(1) = \mathrm{A}, f_{11}(2) = \mathrm{A}, f_{11}(3) = \mathrm{B}, f_{11}(4) = \mathrm{X}$$

Fig. 22 Multiple stereoisogram set of type $(\mathrm{I–I})^2/\mathrm{I}^2$ derived from the oxirane skeleton **5**, where the substitution function f_{11} is applied to Fig. 7. Note that the uppercase letters A, B, and X represent achiral proligands in isolation. where the priority sequence is presumed to be A > B > X

5.4 Promolecules of $\mathrm{A}^2\mathrm{Bp}$

As enumerated in Part I of this series, there are three quadruplets of promolecules having the composition $\mathrm{A}^2\mathrm{Bp}$ (the partition $[\theta]_7$ of Part I) under the action of the

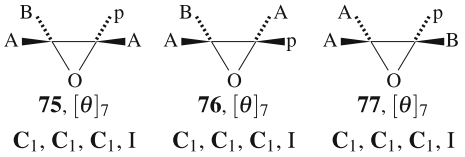

Fig. 23 Three oxiranes with the composition A^2Bp (the partition $[\theta]_7$), each of which is a representative of a quadruplet contained in a type-III stereoisogram. Each of the three oxiranes belongs to an *RS*-stereoisomeric group, a point group, and an *RS*-permutation group, as attached below each promolecule. For the partition $[\theta]_7$, see Part I

RS-stereoisomeric group $\mathbf{C}_{2v\widetilde{\sigma}\widehat{I}}$, where the uppercase letters A and B denote achiral proligands in isolation and the lowercase letter p denotes a chiral proligand in isolation. They are depicted in Fig. 23, where the stereoisogram of each promolecule exhibits type-III.

To discuss the total features of isomerism concerning A^2Bp (partition $[\theta]_7$), the following substitution function is applied to Fig. 7:

$$f_{12} : f_{12}(1) = \mathrm{A},\ f_{12}(2) = \mathrm{A},\ f_{12}(3) = \mathrm{B},\ f_{12}(4) = \mathrm{p}. \tag{31}$$

Thereby, a multiple stereoisogram set of type $(\mathrm{III–III})^2/\mathrm{III}^2$ is generated, as shown in Fig. 24.

The types of component stereoisograms appearing in the symbol $(\mathrm{III–III})^2/\mathrm{III}^2$ are determined by using the flowchart shown in Fig. 9. Thereby, the starting set:

$$\left\{ \frac{\mathbf{75}\ \mathbf{78}}{\mathbf{75}\ \mathbf{78}} \quad \frac{\mathbf{76}\ \mathbf{79}}{\mathbf{76}\ \mathbf{79}} \quad \frac{\mathbf{77}\ \mathbf{80}}{\mathbf{77}\ \mathbf{80}} \right\}. \tag{32}$$

is divided into a final set:

$$\left\{ \left\langle \left(\frac{\mathbf{75}\ \mathbf{78}}{\mathbf{75}\ \mathbf{78}} \right) \left(\frac{\mathbf{76}\ \mathbf{79}}{\mathbf{76}\ \mathbf{79}} \right) \right\rangle \left\langle \left(\frac{\mathbf{77}\ \mathbf{80}}{\mathbf{77}\ \mathbf{80}} \right) \right\rangle \right\}. \tag{33}$$

where each stereoisogram in a pair of parentheses is determined to be type III.

The multiple stereoisogram in the first pair of angle brackets of Eq. 33, which is denoted by the symbol III–III, appears in the top row of the multiple stereoisogram set (Fig. 24). The middle row of Fig. 24 is omitted because it is congruent to the top row. This congruence is denoted by the symbol $(\mathrm{III–III})^2$. The multiple stereoisogram in the second pair of angle brackets of Eq. 33 consists of one pair of parentheses (type III) so that the third row of Fig. 22 degenerates, as shown by the symbol III^2. Hence, the total feature of the multiple stereoisogram set (Fig. 24) is denoted by the symbol $(\mathrm{III–III})^2/\mathrm{III}^2$, as listed in the $[\theta]_7$-row of Table 1.

A pair of *RS*-diastereomers **75/78** is labelled by a pair of stereodescriptors R_a and S_a by using the priority sequence $(\mathrm{A} > \mathrm{B}) \gg (\mathrm{A} > \mathrm{p})$; and another pair of *RS*-diastereomers $\overline{\mathbf{75}}/\overline{\mathbf{78}}$ is labelled by a pair of stereodescriptors S_a and R_a by using the priority sequence $(\mathrm{A} > \mathrm{B}) \gg (\mathrm{A} > \overline{\mathrm{p}})$. Strictly speaking, the two priority sequences are different from each other. In spite of this difference, the stereodescriptors R_a and S_a, which are assigned originally to a pair of *RS*-diastereomers **75/78**, are allowed to be

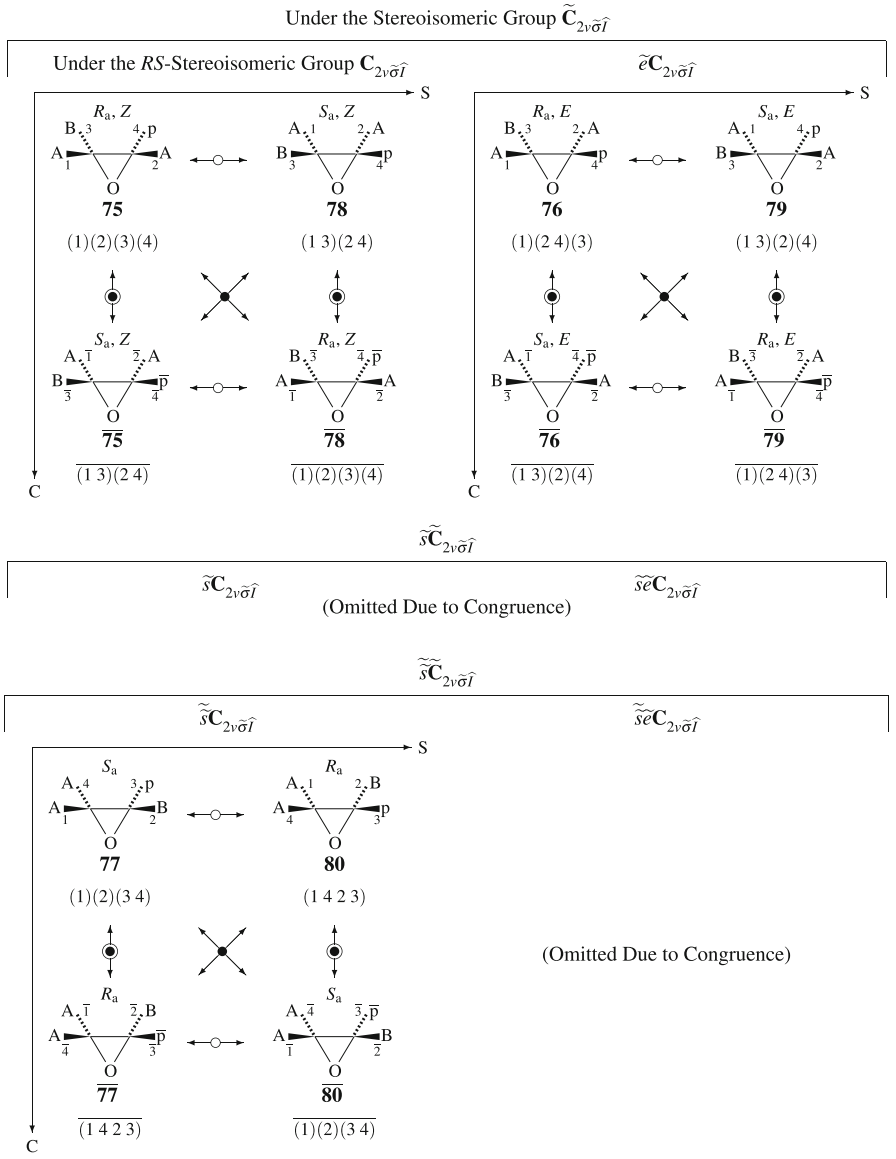

Fig. 24 Multiple stereoisogram set of type $(\mathrm{III}\text{–}\mathrm{III})^2/\mathrm{III}^2$ derived from the oxirane skeleton **5**, where the substitution function f_{12} is applied to Fig. 7. Note that the uppercase letters A and B represent achiral proligands in isolation and the lowercase letters p and $\overline{\mathrm{p}}$ represent chiral proligands with opposite chirality senses. The priority sequence is presumed to be $\mathrm{A} > \mathrm{B} > \mathrm{p} > \overline{\mathrm{p}}$

interpreted to be given to a pair of enantiomers **75/$\overline{\mathbf{75}}$** because of chirality faithfulness (cf. Sect. 6).

Similarly, a pair of **76/79** is labelled by R_a/S_a-stereodescriptors by using $(\mathrm{A} > \mathrm{B}) \gg (\mathrm{A} > \mathrm{p})$ in the application of Rule 1; and another pair of **$\overline{\mathbf{76}}$/$\overline{\mathbf{79}}$** is labelled by

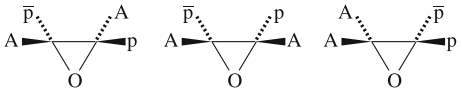

Fig. 25 Three oxiranes with the composition $A^2p\overline{p}$ (the partition $[\theta]_8$), each of which is a representative of a quadruplet contained in a type-I or type-V stereoisogram. Each of the three oxiranes belongs to an *RS*-stereoisomeric group, a point group, and an *RS*-permutation group, as attached below each promolecule. For the partition $[\theta]_8$, see Part I

S_a/R_a-stereodescriptors by using (A > B) ≫ (A > $\overline{p}$) in the application of Rule 1. The stereodescriptors R_a and S_a are allowed to be interpreted to be given to a pair of enantiomers **76/$\overline{\mathbf{76}}$** because of chirality faithfulness (cf. Sect. 6).

Because the different set (a > b) is presumed to have precedence over the equal set (a′ = b′) in the application of Rule 1, a priority sequence (B > p) ≫ (A = A) is used for the promolecule **77** and another priority sequence (B > $\overline{p}$) ≫ (A = A) is used for the promolecule $\overline{\mathbf{77}}$. Thereby a pair of *RS*-diastereomers **77/80** is labelled by a pair of stereodescriptors S_a/R_a; and another pair of *RS*-diastereomers $\overline{\mathbf{77}}/\overline{\mathbf{80}}$ is labelled by a pair of stereodescriptors R_a/S_a. These assignments are used to interpret a pair of enantiomers **77/$\overline{\mathbf{77}}$**.

A pair of *Z/E*-descriptors is given to a pair of *m*-diastereomeric stereoisograms (in a multiple stereoisogram) or to a pair of *ortho*-diastereomers (i.e., **75/76**), i.e., *Z* for **75** etc. and *E* for **76** etc. by using the priority sequence (A > B):(A > p) for Rule 2.

The promolecule **77** or **80** exhibits no assignability of of *Z/E*-descriptors, while it can be labelled by an S_a- or R_a-stereodescriptor.

The partitions $[\theta]_9$ (A^2pq), $[\theta]_{12}$ (ABp^2), $[\theta]_{13}$ ($ABp\overline{p}$), $[\theta]_{16}$($Ap^2\overline{p}$), $[\theta]_{17}$ (Ap^2q), $[\theta]_{24}$ ($p^2\overline{p}q$), $[\theta]_{26}$ ($p^2q\overline{q}$), and $[\theta]_{27}$ (p^2qr) are characterized by multiple stereoisogram sets of type $(III–III)^2/III^2$, so that the assignabilities of stereodescriptors are examined in a similar way, as collected in the corresponding rows of Table 1.

5.5 Promolecules of $A^2p\overline{p}$

As enumerated in Part I of this series, there are three quadruplets of promolecules having the composition $A^2p\overline{p}$ (the partition $[\theta]_8$ of Part I) under the action of the *RS*-stereoisomeric group $\mathbf{C}_{2v\tilde{\sigma}\hat{I}}$, where the uppercase letter A denotes an achiral proligand in isolation and a pair of lowercase letters p/$\overline{p}$ denotes a pair of enantiomeric proligands in isolation. They are depicted in Fig. 25, where the stereoisogram of each promolecule exhibits type-I or type-V.

The total features of isomerism concerning $A^2p\overline{p}$ (partition $[\theta]_8$) are examined by applying the following substitution function to Fig. 7:

$$f_{13} : f_{13}(1) = A,\ f_{13}(2) = p,\ f_{13}(3) = \overline{p},\ f_{13}(4) = A. \tag{34}$$

Thereby, a multiple stereoisogram set of type $(I–V)^2/V^2$ is generated, as shown in Fig. 26.

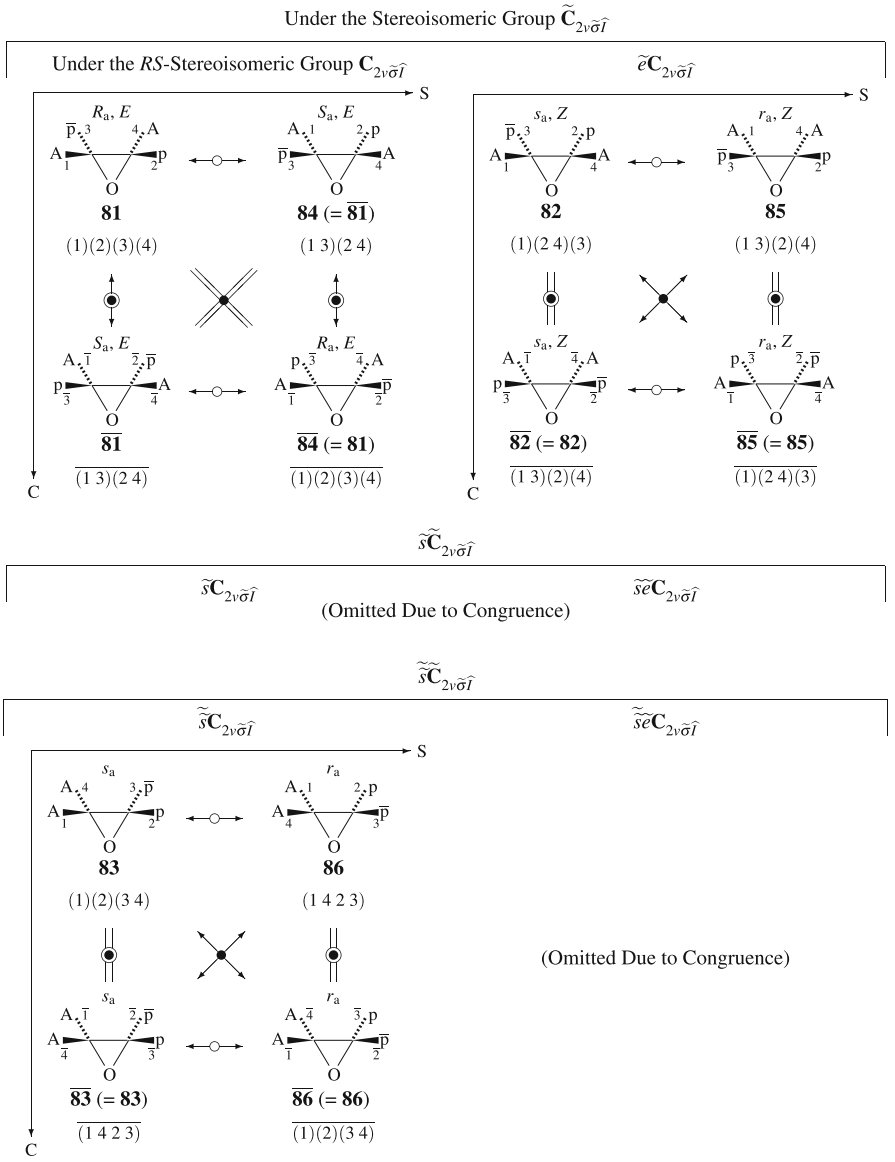

$$f_{13} : f_{13}(1) = \mathrm{A}, f_{13}(2) = \mathrm{p}, f_{13}(3) = \overline{\mathrm{p}}, f_{13}(4) = \mathrm{A}$$

Fig. 26 Multiple stereoisogram set of type $(\mathrm{I–V})^2/\mathrm{V}^2$ derived from the oxirane skeleton **5**, where the substitution function f_{13} is applied to Fig. 7. Note that the uppercase letter A represents an achiral proligand in isolation and the lowercase letters p and $\overline{\mathrm{p}}$ represent chiral proligands with opposite chirality senses. The priority sequence is presumed to be $\mathrm{A} > \mathrm{p} > \overline{\mathrm{p}}$

The types of component stereoisograms appearing in the symbol $(\mathrm{I–V})^2/\mathrm{V}^2$ are determined by using the flowchart shown in Fig. 9. Thereby, the starting set:

$$\left\{ \frac{\mathbf{81}}{\overline{\mathbf{81}}} \quad \mathbf{82\,85} \quad \mathbf{83\,86} \right\}. \tag{35}$$

is divided into a final set:

$$\left\{\left\langle\left(\frac{\mathbf{81}}{\overline{\mathbf{81}}}\right)(\mathbf{82}\ \mathbf{85})\right\rangle\langle(\mathbf{83}\ \mathbf{86})\rangle\right\}, \tag{36}$$

where each stereoisogram in a pair of parentheses is determined to be type-I or type-V.

The multiple stereoisogram in the first pair of angle brackets of Eq. 36, which is denoted by the symbol I–V, appears in the top row of the multiple stereoisogram set (Fig. 26). The middle row of Fig. 26 is omitted because it is congruent to the top row. This congruence is denoted by the symbol $(\text{I–V})^2$. The multiple stereoisogram in the second pair of angle brackets of Eq. 36 consists of one pair of parentheses (type V) so that the bottom row of Fig. 26 degenerates, as shown by the symbol V^2. Hence, the total feature of the multiple stereoisogram set (Fig. 26) is denoted by the symbol $(\text{I–V})^2/\text{V}^2$, as listed in the $[\theta]_8$-row of Table 1.

A pair of *RS*-diastereomers **81/84** is labelled by a pair of stereodescriptors R_a and S_a by using the priority sequence $(\text{A} > \text{p}) \gg (\text{A} > \overline{\text{p}})$ for Rule 1. Because of type I, this assignment is allowed to be interpreted to be given to a pair of enantiomers **81/$\overline{\mathbf{81}}$**.

A pair of *RS*-diastereomers **82/85** is labelled by a pair of stereodescriptors s_a and r_a by using the priority sequence $(\text{A} > \text{p}) \gg (\text{A} > \overline{\text{p}})$ for Rule 1. The lowercase descriptors are used because both **82** and **85** are achiral so that the corresponding stereoisogram is determined to be type V. This case is determined to exhibit extended pseudoasymmetry, which is concerned with the oxirane skeleton **5** (not with a single carbon center). See Sect. 6.4 and refer to [30] for such extended pseudoasymmetry.

A pair of *Z/E*-descriptors is given to a pair of *m*-diastereomeric stereoisograms (in a multiple stereoisogram) or to a pair of *ortho*-diastereomers (i.e., **81/82**), i.e., *E* for **81** etc. and *Z* for **82** etc. by using the priority sequence $(\text{A} > \text{p}):(\text{A} > \overline{\text{p}})$ for Rule 2.

A pair of *RS*-diastereomers **83/86** is labelled by a pair of stereodescriptors s_a and r_a by using the priority sequence $(\text{p} > \overline{\text{p}}) \gg (\text{A} = \text{A})$ for Rule 1. The lowercase descriptors are used because both **83** and **86** are achiral so that the corresponding stereoisogram is determined to be type V. This case is regarded as usual pseudoasymmetry because one ring carbon attached by p and $\overline{\text{p}}$ is an 'pseudoasymmetric carbon' even by means of the conventional terminology.

5.6 Promolecules of $\text{p}^2\overline{\text{p}}^2$

As enumerated in Part I of this series, there are three quadruplets of promolecules having the composition $\text{p}^2\overline{\text{p}}^2$ (the partition $[\theta]_{23}$ of Part I) under the action of the *RS*-stereoisomeric group $\mathbf{C}_{2v\widetilde{\sigma}\widehat{I}}$, where a pair of lowercase letters p/$\overline{\text{p}}$ denotes a pair of enantiomeric proligands in isolation. They are depicted in Fig. 27, where the stereoisogram of each promolecule exhibits type-IV or type-V.

The total features of isomerism concerning $\text{p}^2\overline{\text{p}}^2$ (partition $[\theta]_{23}$) are examined by applying the following substitution function to Fig. 7:

$$f_{14} : f_{14}(1) = \text{p},\ f_{14}(2) = \overline{\text{p}},\ f_{14}(3) = \overline{\text{p}},\ f_{14}(4) = \text{p} \tag{37}$$

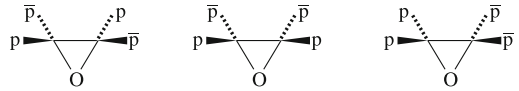

87, $[\theta]_{23}$ **88**, $[\theta]_{23}$ **89**, $[\theta]_{23}$

$\mathbf{C}_{2v}$, $\mathbf{C}_{2v}$, $\mathbf{C}_2$, V $\mathbf{C}_{s\tilde{\sigma}\hat{\sigma}}$, $\mathbf{C}'_s$, $\mathbf{C}_{\tilde{\sigma}}$, IV $\mathbf{C}'_{s\tilde{\sigma}\hat{\sigma}}$, $\mathbf{C}_s$, $\mathbf{C}'_{\tilde{\sigma}}$, IV

Fig. 27 Three oxiranes with the composition $p^2\bar{p}^2$ (the partition $[\theta]_{23}$), each of which is a representative of a quadruplet contained in a type-V or type-IV stereoisogram. Each of the three oxiranes belongs to an *RS*-stereoisomeric group, a point group, and an *RS*-permutation group, as attached below each promolecule. For the partition $[\theta]_{23}$, see Part I

Thereby, a multiple stereoisogram set of type $(\text{V–IV})^2/\text{IV}^2$ is generated, as shown in Fig. 28.

The types of component stereoisograms appearing in the symbol $(\text{V–IV})^2/\text{IV}^2$ are determined by using the flowchart shown in Fig. 9. Thereby, the starting set:

$$\{\mathbf{87\ 90}\quad \mathbf{88}\quad \mathbf{89}\}\,, \tag{38}$$

is divided into a final set:

$$\{\langle(\mathbf{87\ 90})\ (\mathbf{88})\rangle\ \langle(\mathbf{89})\rangle\}\,, \tag{39}$$

where each stereoisogram in a pair of parentheses is determined to be type-IV or type-V.

The multiple stereoisogram in the first pair of angle brackets of Eq. 39, which is denoted by the symbol V–IV, appears in the top row of the multiple stereoisogram set (Fig. 28). The middle row of Fig. 28 is omitted because it is congruent to the top row. This congruence is denoted by the symbol $(\text{V–IV})^2$. The multiple stereoisogram in the second pair of angle brackets of Eq. 39 consists of one pair of parentheses (type IV) so that the bottom row of Fig. 28 degenerates, as shown by the symbol IV^2. Hence, the total feature of the multiple stereoisogram set (Fig. 28) is denoted by the symbol $(\text{V–IV})^2/\text{IV}^2$, as listed in the $[\theta]_{23}$-row of Table 1.

A pair of *RS*-diastereomers **87/90** is labelled by a pair of stereodescriptors r_a and s_a by using the priority sequence $(p > \bar{p}) \gg (p > \bar{p})$ for Rule 1. Because of type V, the lowercase letters r_a and s_a are used to differentiate between the achiral promolecules, i.e., **87** and **90**, both of which exhibit pseudoasymmetry.

An achiral promolecule **88** belongs to type IV, so that it is no assignability of R_a/S_a-stereodescriptors.

A pair of *Z/E*-descriptors is given to a pair of *m*-diastereomeric stereoisograms (in a multiple stereoisogram) or to a pair of *ortho*-diastereomers (i.e., **87/88**). Thereby, we assign *E* to **87** (and **90**) as well as *Z* to **88** by using the priority sequence $(p > \bar{p})$:$(p > \bar{p})$ for Rule 2.

An achiral promolecule **89** belongs to type IV, so that it exhibits no assignability of R_a/S_a-stereodescriptors. The achiral promolecule **89** exhibits no *cis/trans*-isomerism, so as not to be differentiated by *Z/E*-descriptors.

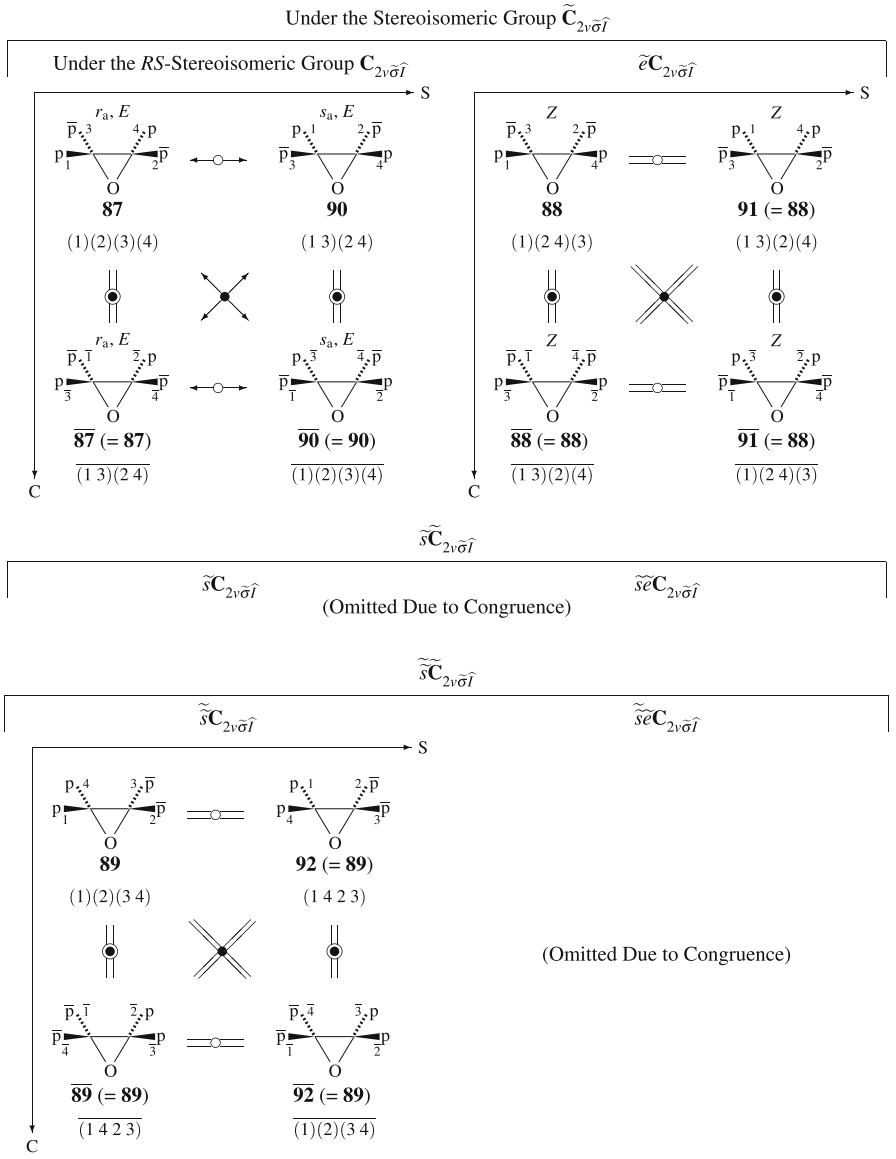

$$f_{14} : f_{14}(1) = \mathrm{p}, f_{14}(2) = \overline{\mathrm{p}}, f_{14}(3) = \overline{\mathrm{p}}, f_{14}(4) = \mathrm{p}$$

Fig. 28 Multiple stereoisogram set of type $(\mathrm{V\text{–}IV})^2/\mathrm{IV}^2$ derived from the oxirane skeleton **5**, where the substitution function f_{14} is applied to Fig. 7. Note that the lowercase letters p and $\overline{\mathrm{p}}$ represent chiral proligands with opposite chirality senses. The priority sequence is presumed to be $\mathrm{p} > \overline{\mathrm{p}}$

6 Chirality faithfulness

6.1 Chirality faithfulness versus reflection invariance

The Cahn-Ingold-Prelog (CIP) system presumes a double criterion in the assignment of *R/S*-stereodescriptors: A pair of *R/S*-stereodescriptors is given to a pair of enantiomers which are concerned with 'chirality units', while it is given to a pair of diastereomers which are concerned with 'pseudoasymmetric units' [1,2,4]. The lowercase labels *r* and *s* are used for specifying 'pseudoasymmetric units' by the coinage of the term 'reflection-invariant' [2]. Note that the determination based on the term 'reflection-invariant' emphasizes enantiomeric relationships and implicitly nullifies the participation of *RS*-diastereomeric relationships.

In contrast, the stereoisogram approach has adopted the concept of *chirality faithfulness* [31] to rationalize the assignment of lowercase labels, where the chirality faithfulness are concerned with how stereodescriptors assigned originally by *RS*-diastereomeric relationships are applied to the description of enantiomeric relationships. In case of tetrahedral promolecules, priority permutations are introduced as a convenient device for determining chirality faithfulness [14]. The determination in terms of priority permutations [14], however, are not applicable to the present cases of oxirane promolecules, because the R_a/S_a-stereodescriptors of the present article exhibit different features from the *R/S*-stereodescriptors for tetrahedral promolecules.

To discuss whether or not stereoisograms of type I, type III, or type V require lowercase labels, we focus our attention on the reference promolecule and its holantimeric promolecule in the diagonal direction of the stereoisograms, e.g., **7** and $\overline{\mathbf{13}}$ (= **7**) for a type-I stereoisogram shown in Fig. 4(a) as well as **46** and $\overline{\mathbf{52}}$ (= **52**) for a type-V stereoisogram shown in shown in Fig. 16. Thereby, a stereoisogram of type I, type III, or type V contains two *RS*-diastereomeric relationships along the horizontal direction, where one is called a *proper RS-diastereomeric relationship* (concerning the reference promolecule) and the other is called an *improper RS-diastereomeric relationship* (concerning the corresponding holantimer). For example, the type-I stereoisogram shown in Fig. 4(a) contains a proper *RS*-diastereomeric relationship between **7** and **13** and an improper *RS*-diastereomeric relationship between $\overline{\mathbf{13}}$ and $\overline{\mathbf{7}}$. The type-V stereoisogram shown in the upper-right position of Fig. 16 contains a proper *RS*-diastereomeric relationship between **46** and **52** and an improper *RS*-diastereomeric relationship between $\overline{\mathbf{52}}$ and $\overline{\mathbf{46}}$.

In a type-I stereoisogram, in general, the reference promolecule (e.g., **7**) and its holantimeric promolecule (e.g., $\overline{\mathbf{13}}$) are identical with each other, so that they have a common stereodescriptor, R_a (or S_a). As a result, the proper *RS*-diastereomeric relationship coincides with the improper *RS*-diastereomeric relationship in the type-I stereoisogram. It means that a pair of R_a/S_a-stereodescriptors is assigned parallel to the proper and improper *RS*-diastereomeric relationships. Although type-III stereoisograms do not exhibit such coincidence, the proper *RS*-diastereomeric relationship may be parallel to the improper *RS*-diastereomeric relationship during the assignment of R_a/S_a-stereodescriptors in some type-III stereoisograms. As a result, the term *chirality-faithful* is defined to comprehend type-I and type-III stereoisograms:

Definition 1 (Chirality-faithful absolute configurations) If the stereodescriptor of a reference promolecule, R_a (or S_a), is identical with that of its holantimer, R_a (or S_a), this case is referred to as being *chirality-faithful* and characterized by uppercase labels.

If chirality-faithful, the pairwise assignment based on the proper *RS*-diastereomeric relationship is parallel to the pairwise assignment based on the improper *RS*-diastereomeric relationship. It follows that a pair of *R/S*-stereodescriptors originally based on the proper *RS*-diastereomeric relationship is allowed to be interpreted to be given to the enantiomeric relationship. This allowed interpretation is also referred to as being chirality-faithful, so that the *R/S*-stereodescriptors are designated in uppercase labels.

On the other hand, the term *chirality-unfaithful* is defined to comprehend type-V and some type-III stereoisograms:

Definition 2 (Chirality-unfaithful absolute configurations) If the stereodescriptor of a reference promolecule, R_a (or S_a), is opposite to that of its holantimer, S_a (or R_a), this case is referred to as being *chirality-unfaithful* and characterized by lowercase labels.

If chirality-unfaithful, the pairwise assignment based on the proper *RS*-diastereomeric relationship is anti-parallel to the pairwise assignment based on the improper *RS*-diastereomeric relationship. It follows that a pair of *R/S*-stereodescriptors originally based on the proper *RS*-diastereomeric relationship is not allowed to be interpreted to be given to the enantiomeric relationship. This forbidden interpretation is also referred to as being chirality-unfaithful, so that the *R/S*-stereodescriptors are designated in lowercase labels.

It is to be added that the term *chirality-unfaithful* is capable of deducing the conventional term 'reflection-invariant', while the term 'reflection-invariant' is incapable of deducing the present term *chirality-unfaithful*. This is because the conventional term 'reflection-invariant' lacks the concepts of *RS*-diastereomeric relationships and *RS*-stereogenicity.

6.2 Chirality-faithful cases

6.2.1 Type-I cases

Let us apply the following substitution function to Fig. 7:

$$f_{15} : f_{15}(1) = \mathrm{A},\ f_{15}(2) = \mathrm{B},\ f_{15}(3) = \mathrm{A},\ f_{15}(4) = \mathrm{A}, \tag{40}$$

which corresponds to the composition $\mathrm{A}^3\mathrm{B}$ (the partition $[\theta]_2$). The resulting multiple stereoisogram set of type $(\mathrm{I}^2)^3$ degenerates into one stereoisogram of type I shown in Fig. 29.

A pair of *RS*-diastereomers **93/94** is labelled by a pair of stereodescriptors R_a and S_a, where the priority sequence $(\mathrm{A} > \mathrm{B}) \gg (\mathrm{A} = \mathrm{A})$ is used for the application of Rule 1. Because of type I, the *RS*-diastereomeric relationship between **93** and **94** coalesces

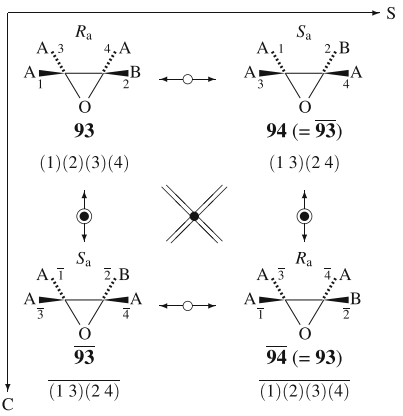

Fig. 29 Multiple stereoisogram set of type $(I^2)^3$ derived from the oxirane skeleton **5**, where the substitution function f_{15} is applied to Fig. 7. The multiple stereoisogram set degenerates to give a stereoisogram type I. Note that the uppercase letters A and B represent achiral proligands, where the priority sequence is presumed to be A > B. This is a chirality-faithful case

$$f_{15} : f_{15}(1) = \mathrm{A}, f_{15}(2) = \mathrm{B}, f_{15}(3) = \mathrm{A}, f_{15}(4) = \mathrm{A}$$

to the enantiomeric relationship between **93** and $\overline{\mathbf{93}}$. Hence, a pair of stereodescriptors R_a and S_a, which is originally assigned to *RS*-diastereomers **93/94**, is interpreted to be assigned to a pair of enantiomers **93** and $\overline{\mathbf{93}}$. This case is an example of a chirality-faithful assignment, because the reference promolecule **93** and its holantimer **94** have an identical uppercase label R_a.

In general, the assignment of R_a/S_a-stereodescriptors to a stereoisogram of type I is determined to be chirality-faithful. Each stereoisogram of the multiple stereoisogram set of type I–I/I–I/I–I (Fig. 8) is determined to be chirality-faithful. For example, both **7** and its holantimer $\overline{\mathbf{13}}$ (= **7**) are characterized by the stereodescriptor *R*, because the priority sequence $(\mathrm{A}(1) > \mathrm{X}(3)) \gg (\mathrm{B}(2) > \mathrm{Y}(4))$ for **7** is converted into $(\mathrm{A}(\overline{1}) > \mathrm{X}(\overline{3})) \gg (\mathrm{B}(\overline{2}) > \mathrm{Y}(\overline{4}))$ for $\overline{\mathbf{13}}$ on the action of a reflection.

The multiple stereoisogram set of type $(\mathrm{I–V})^2/\mathrm{V}^2$ (Fig. 26) contains a stereoisogram of type I for **81**, where the priority sequence $(\mathrm{A}(4) > \mathrm{p}(2)) \gg (\mathrm{A}(1) > \overline{\mathrm{p}}(3))$ for **81** is converted into $(\mathrm{A}(\overline{1}) > \mathrm{p}(\overline{3})) \gg (\mathrm{A}(\overline{4}) > \overline{\mathrm{p}}(\overline{2}))$ for $\overline{\mathbf{84}}$ on the action of a reflection. This conversion apparently causes no change of alignment, if the numbering of positions is disregarded. Hence, this conversion results in the assignment of the same label *R* to both **81** and its holantimer $\overline{\mathbf{84}}$, which is concluded to be the chirality-faithful assignment.

6.2.2 Chirality-faithful Type-III cases

Let us apply the following substitution function to Fig. 7:

$$f_{16} : f_{16}(1) = \mathrm{A}, f_{16}(2) = \mathrm{p}, f_{16}(3) = \mathrm{A}, f_{16}(4) = \mathrm{A}, \tag{41}$$

which corresponds to the composition $\mathrm{A}^3\mathrm{p}$ (the partition $[\theta]_3$). The resulting multiple stereoisogram set of type $(\mathrm{III}^2)^3$ degenerates into one stereoisogram of type III shown in Fig. 30.

A pair of **95/96** in a proper *RS*-diastereomeric relationship is labelled by a pair of stereodescriptors R_a and S_a, where the priority sequence $(\mathrm{A} > \mathrm{p}) \gg (\mathrm{A} = \mathrm{A})$ is used

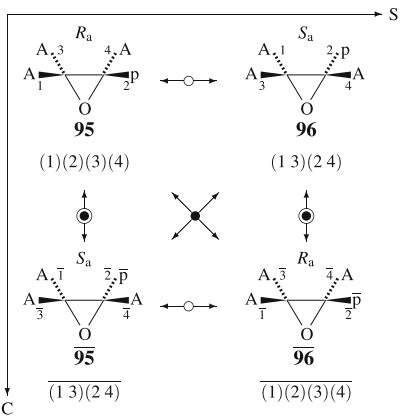

Fig. 30 Multiple stereoisogram set of type $(\mathrm{III}^2)^3$ derived from the oxirane skeleton **5**, where the substitution function f_{16} is applied to Fig. 7. The multiple stereoisogram set degenerates to give a single stereoisogram of type III. Note that the uppercase letter A represents an achiral proligand and a pair of lowercase letters p/$\overline{\mathrm{p}}$ represents a pair of enantiomeric proligands in isolation. where the priority sequence is presumed to be A > p > $\overline{\mathrm{p}}$. This is a chirality-faithful case

$$f_{16} : f_{16}(1) = \mathrm{A}, f_{16}(2) = \mathrm{p}, f_{16}(3) = \mathrm{A}, f_{16}(4) = \mathrm{A}$$

for the application of Rule 1. Another pair of $\overline{\mathbf{96}}/\overline{\mathbf{95}}$ in an improper *RS*-diastereomeric relationship is labelled by a pair of stereodescriptors R_a and S_a, where the priority sequence $(\mathrm{A} > \overline{\mathrm{p}}) \gg (\mathrm{A} = \mathrm{A})$ is used for the application of Rule 1. As a result, this case is concluded to be chirality-faithful. Although the priority sequences $(\mathrm{A} > \mathrm{p}) \gg (\mathrm{A} = \mathrm{A})$ and $(\mathrm{A} > \overline{\mathrm{p}}) \gg (\mathrm{A} = \mathrm{A})$ are different, a pair of stereodescriptors R_a and S_a, which is originally assigned to *RS*-diastereomers **95/96**, is interpreted to be assigned to a pair of enantiomers **95** and $\overline{\mathbf{95}}$.

Parallel examinations applied to the compositions Ap^3 (partition $[\theta]_{15}$) and $\mathrm{p}^3\mathrm{q}$ (partition $[\theta]_{22}$) reveal that they are chirality-faithful cases.

6.3 Chirality-unfaithful cases

6.3.1 Type-V cases

Type-V stereoisograms exhibit chirality unfaithfulness. For example, the multiple stereoisogram set of type $(\mathrm{I–V})^2/\mathrm{V}^2$ (Fig. 26) contains a stereoisogram of type V for **83**, where a pair of **83/86** in a proper *RS*-diastereomeric relationship is labelled to have a pair of $s_\mathrm{a}/r_\mathrm{a}$ by using the priority sequence $(\mathrm{p}(2) > \overline{\mathrm{p}}(3)) \gg (\mathrm{A}(1) = \mathrm{A}(4))$. Another pair of $\overline{\mathbf{86}}/\overline{\mathbf{83}}$ in an improper *RS*-diastereomeric relationship is labelled to have a pair of $r_\mathrm{a}/s_\mathrm{a}$ by using the priority sequence $(\mathrm{p}(\overline{3}) > \overline{\mathrm{p}}(\overline{2})) \gg (\mathrm{A}(\overline{1}) = \mathrm{A}(\overline{4}))$. The opposite labelling of **83** (s_a) and its holantimer $\overline{\mathbf{86}}$ (r_a) shows that this case is chirality-unfaithful. The lowercase labels are used to emphasize the chirality unfaithfulness. It should be noted that both **83** and **86** are achiral so as to exhibit pseudoasymmetry.

6.3.2 Chirality-unfaithful type-III cases

Let us apply the following substitution function to Fig. 7:

$$f_{17} : f_{17}(1) = \mathrm{p},\ f_{17}(2) = \mathrm{p},\ f_{17}(3) = \mathrm{p},\ f_{17}(4) = \overline{\mathrm{p}}, \tag{42}$$

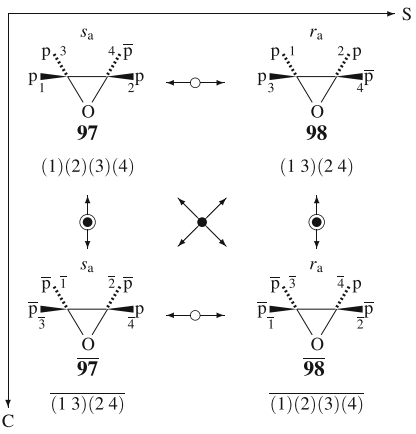

Fig. 31 Multiple stereoisogram set of type $(\mathrm{III}^2)^3$ derived from the oxirane skeleton **5**, where the substitution function f_{17} is applied to Fig. 7. The multiple stereoisogram set degenerates to give a single stereoisogram of type III. Note that a pair of lowercase letters p/$\overline{\mathrm{p}}$ represents a pair of enantiomeric proligands in isolation. The priority sequence is presumed to be p > $\overline{\mathrm{p}}$. This is a chirality-unfaithful case

$$f_{17} : f_{17}(1) = \mathrm{p}, f_{17}(2) = \mathrm{p}, f_{17}(3) = \mathrm{p}, f_{17}(4) = \overline{\mathrm{p}}$$

which corresponds to the composition $\mathrm{p}^3\overline{\mathrm{p}}$ (the partition $[\theta]_{21}$). The resulting multiple stereoisogram set of type $(\mathrm{III}^2)^3$ degenerates into one stereoisogram of type III shown in Fig. 31.

A pair of **97/98** in a proper *RS*-diastereomeric relationship is labelled by a pair of stereodescriptors s_a and r_a, where the priority sequence $(\mathrm{p} > \overline{\mathrm{p}}) \gg (\mathrm{p} = \mathrm{p})$ is used for the application of Rule 1. Another pair of $\overline{\mathbf{98}}/\overline{\mathbf{97}}$ in an improper *RS*-diastereomeric relationship is labelled by a pair of stereodescriptors r_a and s_a, where the priority sequence $(\mathrm{p} > \overline{\mathrm{p}}) \gg (\overline{\mathrm{p}} = \overline{\mathrm{p}})$ is used for the application of Rule 1. The opposite assignment of a reference promolecule **97** (s_a) and its holantimer $\overline{\mathbf{98}}$ (r_a) shows that this case is chirality-unfaithful. The lowercase labels are used to emphasize the chirality unfaithfulness. A pair of stereodescriptors r_a and s_a, which is originally assigned to *RS*-diastereomers **97/98**, cannot be interpreted to be assigned to a pair of enantiomers $\mathbf{97}/\overline{\mathbf{97}}$.

6.3.3 Alternation of chirality faithfulness

Let us apply the following substitution function to the first reference stereoisogram of Fig. 7:

$$f_{18} : f_{18}(1) = \mathrm{A}, f_{18}(2) = \mathrm{p}, f_{18}(3) = \mathrm{B}, f_{18}(4) = \overline{\mathrm{p}}, \tag{43}$$

which corresponds to the composition $\mathrm{ABp}\overline{\mathrm{p}}$ (the partition $[\theta]_{13}$). Although the corresponding multiple stereoisogram set can be drawn in a similar way to the multiple stereoisogram set of type $(\mathrm{III}–\mathrm{III})^2/\mathrm{III}^2$ (Fig. 24), it is characterized to be type $(\mathrm{III}–\mathrm{III})^2/\mathrm{III}=\mathrm{III}$, because the degenerate III=III part exhibits a special feature (see the next subsection). Among the stereoisograms contained in the resulting multiple stereoisogram set of type $(\mathrm{III}–\mathrm{III})^2/\mathrm{III}=\mathrm{III}$, the stereoisogram shown in Fig. 32 depicts the part III=III.

If we adopt the priority sequence $(\mathrm{A} > \mathrm{B}) \gg (\mathrm{p} > \overline{\mathrm{p}})$, the same label R_a is assigned to the reference promolecule **99** and its holantimer $\overline{\mathbf{100}}$. Hence, a pair of stereodescriptors

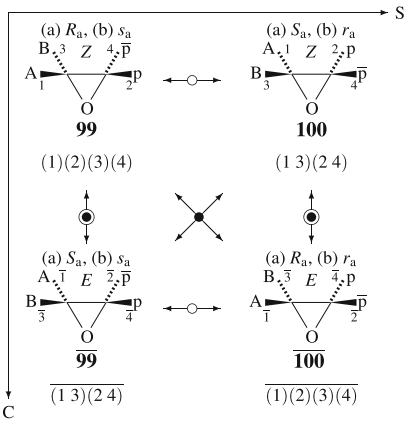

$$f_{18} : f_{18}(1) = \mathrm{A}, f_{18}(2) = \mathrm{p}, f_{18}(3) = \mathrm{B}, f_{18}(4) = \overline{\mathrm{p}}$$

Fig. 32 Stereoisogram of type III selected from the III=III part of an multiple stereoisogram set of type (III–III)^2/III=III, where the substitution function f_{18} is applied to the first reference stereoisogram shown in Fig. 7. Note that the uppercase letters A and B represent achiral proligands in isolation and a pair of lowercase letters p/$\overline{\mathrm{p}}$ represents a pair of enantiomeric proligands in isolation. **a** The priority sequence is presumed to be (A > B) $\gg$ (p > $\overline{\mathrm{p}}$) so as to exemplify a chirality-faithful case. **b** The priority sequence is presumed to be (p > $\overline{\mathrm{p}}$) $\gg$ (A > B) so as to exemplify a chirality-unfaithful case

R_a and S_a, which is originally assigned to *RS*-diastereomers **99/100**, is interpreted to be assigned to a pair of enantiomers **99** and $\overline{\mathbf{99}}$. This is a chirality-faithful case so as to give uppercase labels (case (a) in Fig. 32).

On the other hand, if we adopt the priority sequence (p > $\overline{\mathrm{p}}$) $\gg$ (A > B), the label s_a is assigned to the reference promolecule **99**, while the opposite label r_a is assigned to its holantimer $\overline{\mathbf{100}}$. Hence, a pair of stereodescriptors s_a and r_a, which is originally assigned to *RS*-diastereomers **99/100**, cannot be interpreted to be assigned to a pair of enantiomers **99** and $\overline{\mathbf{99}}$. In fact, the label for **99** (s_a) is identical with the label for $\overline{\mathbf{99}}$ (s_a). This is a chirality-unfaithful case so as to give lowercase labels (case (b) in Fig. 32).

6.3.4 So-called 'Geometric Enantiomers'

Geometrically speaking, the III=III part of the multiple stereoisogram set of type (III–III)^2/III=III (Fig. 32) exhibits a special feature. Thus, the reference promolecule **99** (or its *RS*-diastereomer **100**) is labelled by a *Z*-descriptor. On the other hand, its enantiomer $\overline{\mathbf{99}}$ (or its holantimer $\overline{\mathbf{100}}$) is labelled by an *E*-descriptor. Hence, the pair of enantiomers **99** and $\overline{\mathbf{99}}$ can be characterized by *Z*/*E*-descriptors. This case should be regarded as a special case in which an enantiomeric relationship coincides with an *ortho*-diastereomeric relationship. In fact, the application of the substitution function f_{18} to the numbered skeleton **16** (produced by (1 3)(2)(4), cf. Fig. 7) generates a promolecule identical with $\overline{\mathbf{99}}$, which is generated by the application of the substitution function f_{18} to the numbered skeleton $\overline{\mathbf{5}}$ (produced by $\overline{(1\ 3)(2\ 4)}$, cf. Fig. 7). It follows that the coincidence is represented by the symbol III=III in place of III^2. In spite of the coincidence, the *Z*/*E*-descriptors are permitted to characterize the stereoisomerism

between **99** and $\overline{\mathbf{99}}$. Note that chirality is independent of stereoisomerism specified by *Z/E*-descriptors, just as chirality is independent of *RS*-stereogenicity specified by *R/S*-stereodescriptors of the CIP system.

Each symbol Y with an asterisk in the (assignability-of-*Z/E*)-column of Table 1 shows an example which exhibits such a special feature as described for the *Z/E*-descriptors of Fig. 32. Note that each example contains a pair of p/$\overline{\text{p}}$ on one carbon atom of the oxirane skeleton.

The *Z/E*-descriptors for the stereoisogram shown in Fig. 32 exhibit a similar feature to 'geometric enantiomers' described for double bonds. For the term 'geometric enantiomers', see Section 1.1.2.2.3 of [4], where enantiomeric relationships are regarded to have precedence over *Z/E*-isomerism. See also Section 2–4 of [32]. In a similar way to the present case of Fig. 32, however, *Z/E*-descriptors are permitted to characterize the stereoisomerism for 'geometric enantiomers'. In other words, **99** and $\overline{\mathbf{99}}$ is enantiomeric and at the same time *Z/E*-isomeric (diastereomeric, conventionally speaking), where the conventional dichotomy between enantiomers and diastereomers cannot be maintained. This point has been discussed in a previous paper by the present author [17]. It should be again emphasized that chirality is independent of stereoisomerism specified by *Z/E*-descriptors, just as chirality is independent of *RS*-stereogenicity specified by *R/S*-stereodescriptors.

6.4 Extended pseudoasymmetry

In this article, the term *pseudoasymmetry* or *extended pseudoasymmetry* is concerned with type-V stereoisograms. Note that the term *chirality-unfaithful* is concerned with type-V stereoisograms or some type-III stereoisograms.

Let us compare the two stereoisograms contained in the multiple stereoisogram set of type $(\text{I–V})^2/\text{V}^2$ (Fig. 26). The pseudoasymmetry of the achiral promolecules **83** and **86**, which is shown in a stereoisogram of type V (the third stereoisogram of Fig. 26), stems from a pair of p/$\overline{\text{p}}$ attaching to a carbon atom (so-called 'a pseudoasymmetric carbon'). This is akin to the pseudoasymmetry to a tetrahedral skeleton.

On the other hand, the second stereoisogram of type V shown in Fig. 26 exhibits another type of pseudoasymmetry called *extended pseudoasymmetry*, which is based on an oxirane skeleton, not on a so-called 'a pseudoasymmetric carbon'. In this stereoisogram, a pair of **82/85** in a proper *RS*-diastereomeric relationship is labelled to have a pair of s_a/r_a by using the priority sequence $(\text{A}(4) > \text{p}(2)) \gg (\text{A}(1) > \overline{\text{p}}(3))$. Another pair of $\overline{\mathbf{85}}/\overline{\mathbf{82}}$ in an improper *RS*-diastereomeric relationship is labelled to have a pair of r_a/s_a by using the priority sequence $(\text{A}(\overline{1}) > \text{p}(\overline{3})) \gg (\text{A}(\overline{4}) > \overline{\text{p}}(\overline{2}))$. The opposite labelling of **82** (s_a) and its holantimer $\overline{\mathbf{85}}$ (r_a) shows that this case is chirality-unfaithful. The lowercase labels are used to emphasize the chirality unfaithfulness.

The multiple stereoisogram set of type I–V/I–V/V–V shown in Fig. 16 provides us with further examples of pseudoasymmetry and extended pseudoasymmetry. The stereoisogram of type V containing **46** and **52** exhibits extended pseudoasymmetry; and the stereoisogram of type V containing **48** and **54** exhibits extended pseudoasymmetry. On the other hand, the stereoisogram of type V containing **49** and **55** exhibits

pseudoasymmetry; and the stereoisogram of type V containing **50** and **56** exhibits pseudoasymmetry.

7 Conclusion

In order to discuss geometric and stereoisomeric properties of oxirane derivatives, the *RS*-stereoisomeric group $\mathbf{C}_{2v\tilde{\sigma}\hat{I}}$ (order 8) is defined by starting from the point group $\mathbf{C}_{2v}$ (order 4), where point groups for chirality (or enantiomeric relationships), *RS*-permutation groups for *RS*-stereogenicity (or *RS*-diastereomeric relationships), and ligand-reflection groups for sclerality (or holantimeric relationships) are integrated in a consistent way. Stereoisograms of type I to V are introduced as graphic representations of *RS*-stereoisomeric groups. Then the *cis/trans*- or *Z/E*-isomerism is characterized by the stereoisomeric group $\widetilde{\mathbf{C}}_{2v\tilde{\sigma}\hat{I}}$ (order 16). Multiple stereoisograms are introduced as graphic representations of stereoisomeric groups. Finally, the total features of isomerism based on an oxirane skeleton is characterized by the isoskeletal group $\widetilde{\widetilde{\mathbf{C}}}_{2v\tilde{\sigma}\hat{I}}$ (order 48). Multiple stereoisogram sets are introduced as graphic representations of isoskeletal groups. Thereby, *RS*-stereoisomers, *Z/E*-isomers, and isoskeletal isomers are classified by means of equivalence classes based on these groups, where flowcharts for determining types of multiple stereoisogram sets are proposed. A new system of notations by R_a/S_a-descriptors is proposed to specify absolute configurations of oxirane derivatives. The notation system of specifying *Z/E*-descriptors is modified to be applicable to oxirane derivatives. Thereby, promolecules of ABXp and $\mathrm{p\bar{p}q\bar{q}}$ are examined as examples for non-degenerate cases. On the other hand, promolecules of $\mathrm{A^2B^2}$, $\mathrm{A^2p^2}$, $\mathrm{A^2BX}$, $\mathrm{A^2Bp}$, $\mathrm{A^2p\bar{p}}$, and $\mathrm{p^2\bar{p}^2}$ are examined as examples for degenerate cases. The concept of *chirality faithfulness* is revised to give a rational judgement on whether R_a/S_a-stereodescriptors are labelled in uppercase or lowercase letters. Pseudoasymmetry and extended pseudoasymmetry are discussed on the basis of type-V stereoisograms.

References

1. R.S. Cahn, C.K. Ingold, V. Prelog, Angew. Chem. Int. Ed. Eng. **5**, 385–415 (1966)
2. V. Prelog, G. Helmchen, Angew. Chem. Int. Ed. Eng. **21**, 567–583 (1982)
3. IUPAC Chemical Nomenclature and Structure Representation Division, Provisional Recommendations. Nomenclature of Organic Chemistry, (2004). http://www.iupac.org/reports/provisional/abstract04/favre_310305.html
4. G. Helmchen, A. General Aspects. 1. Nomenclature and Vocabulary of Organic Stereochemistry, in *Stereoselective Synthesis. Methods of Organic Chemistry (Houben-Weyl). Workbench Edition E21*, 4 ed., ed. by G. Helmchen, R. W. Hoffmann, J. Mulzer, and E. Schaumann, Georg Thieme, vol. 1 (Stuttgart New York, 1996), p. 1–74
5. N.G. Connelly, T. Damhus, R.M. Hartshorn, A.T. Hutton, and IUPAC, *Nomenclature of Inorganic Chemistry, IUPAC Recommendations 2005* (RSC Publishing, Cambridge, 2005)
6. IUPAC Organic Chemistry Division, Pure Appl. Chem. **68**, 2193–2222 (1996)
7. S. Fujita, Stereoisograms: A Remedy Against Oversimplified Dichotomy between Enantiomers and Diastereomers in Stereochemistry, in *Chemical Information and Computational Challenge in the 21st Chentury*, ed. by M. V. Putz, Nova, New York (2012) Chapter 9, p. 223–242
8. S. Fujita, J. Org. Chem. **69**, 3158–3165 (2004)
9. S. Fujita, J. Math. Chem. **35**, 265–287 (2004)

10. S. Fujita, Tetrahedron **60**, 11629–11638 (2004)
11. S. Fujita, MATCH Commun. Math. Comput. Chem. **54**, 39–52 (2005)
12. S. Fujita, J. Math. Chem. **52**, 508–542 (2014)
13. S. Fujita, J. Math. Chem. **52**, 543–574 (2014)
14. S. Fujita, J. Math. Chem. **52**, 1514–1534 (2014)
15. S. Fujita, MATCH Commun. Math. Comput. Chem. **52**, 3–18 (2004)
16. S. Fujita, Memoirs of the faculty of engineering and design. Kyoto Inst. Technol. **53**, 19–38 (2005)
17. S. Fujita, J. Chem. Inf. Comput. Sci. **44**, 1719–1726 (2004)
18. S. Fujita, MATCH Commun. Math. Comput. Chem. **53**, 147–159 (2005)
19. S. Fujita, MATCH Commun. Math. Comput. Chem. **71**, 511–536 (2014)
20. S. Fujita, MATCH Commun. Math. Comput. Chem. **71**, 537–574 (2014)
21. S. Fujita, MATCH Commun. Math. Comput. Chem. **71**, 575–608 (2014)
22. K. Mislow, Bull. Soc. Chim. Belg. **86**, 595–601 (1977)
23. K.A. Black, J. Chem. Educ. **67**, 141–142 (1990)
24. A. von Zelewsky, *Stereochemistry of Coordination Compounds* (Wiley, Chichester, 1996)
25. M.J.T. Ronbinson, *Organic Stereochemistry* (Oxford University, Oxford, 2000)
26. http://en.wkipedia.org/wiki/Isomer
27. J.E. Blackwood, C.L. Gladys, K.L. Loening, A.E. Petrarca, J.E. Rush, J. Am. Chem. Soc. **90**, 509–510 (1968)
28. J.E. Blackwood, C.L. Gladys, A.E. Petrarca, W.H. Powell, J.E. Rush, J. Chem. Doc. **8**, 30–32 (1968)
29. The Commission on the Nomenclature of Organic Chemistry of IUPAC, Pure App. Chem. **45**, 11–30 (1976)
30. S. Fujita, Tetrahedron: Asymmetry **23**, 623–634 (2012)
31. S. Fujita, J. Comput. Aided Chem. **10**, 16–29 (2009)
32. K. Mislow, *Introduction to Stereochemistry* (Benjamin, New York, 1965)